

15. Gaynor JJ, Feuer EJ, Tan CC, et al. On the use of cause-specific failure and conditional failure probabilities: examples from clinical oncology data. *J Am Stat Assoc.* 1993; **88**: 400–9.
16. Sacks D, McClenny TE, Cardella JF, Lewis CA. Society of interventional radiology clinical practice guidelines. *J Vasc Interv Radiol.* 2003; **14**: S199–202.
17. Lencioni R, Caramella D, Bartolozzi C. Response of hepatocellular carcinoma to percutaneous ethanol injection: CT and MR evaluation. *J Comput Assist Tomogr.* 1993; **17**: 723–9.
18. Lin SM, Lin CJ, Lin CC, Hsu CW, Chen YC. Radiofrequency ablation improves prognosis compared with ethanol injection for hepatocellular carcinoma < or = 4 cm. *Gastroenterology.* 2004; **127**: 1714–23.
19. Sala M, Llovet JM, Vilana R, et al. Initial response to percutaneous ablation predicts survival in patients with hepatocellular carcinoma. *Hepatology.* 2004; **40**: 1352–60.
20. Llovet JM, Fuster J, Bruix J. Intention-to-treat analysis of surgical treatment for early hepatocellular carcinoma: resection versus transplantation. *Hepatology.* 1999; **30**: 1434–40.
21. Minagawa M, Makuuchi M, Takayama T, Kokudo N. Selection criteria for repeat hepatectomy in patients with recurrent hepatocellular carcinoma. *Ann Surg.* 2003; **238**: 703–10.
22. Poon RT, Fan ST, Lo CM, Liu CL, Wong J. Long-term survival and pattern of recurrence after resection of small hepatocellular carcinoma in patients with preserved liver function: implications for a strategy of salvage transplantation. *Ann Surg.* 2002; **235**: 373–82.
23. Johnson P, Bruix J. Hepatocellular carcinoma and the art of prognostication. *J Hepatol.* 2000; **33**: 1006–8.
24. Di Stasi M, Buscarini L, Livraghi T, et al. Percutaneous ethanol injection in the treatment of hepatocellular carcinoma. A multicenter survey of evaluation practices and complication rates. *Scand J Gastroenterol.* 1997; **32**: 1168–73.
25. Capussotti L, Muratore A, Amisano M, et al. Liver resection for hepatocellular carcinoma on cirrhosis: analysis of mortality, morbidity and survival—a European single center experience. *Eur J Surg Oncol.* 2005; **31**: 986–93.
26. Taketomi A, Kitagawa D, Itoh S, et al. Trends in morbidity and mortality after hepatic resection for hepatocellular carcinoma: an institute's experience with 625 patients. *J Am Coll Surg.* 2007; **204**: 580–7.
27. Imamura H, Seyama Y, Kokudo N, et al. One thousand fifty-six hepatectomies without mortality in 8 years. *Arch Surg.* 2003; **138**: 1198–206; discussion 206.
28. Shiina S, Tateishi R, Arano T, et al. Radiofrequency ablation for hepatocellular carcinoma: 10-year outcome and prognostic factors. *Am J Gastroenterol.* 2012; **107**: 569–77.
29. Lin SM, Lin CJ, Lin CC, Hsu CW, Chen YC. Randomised controlled trial comparing percutaneous radiofrequency thermal ablation, percutaneous ethanol injection, and percutaneous acetic acid injection to treat hepatocellular carcinoma of 3 cm or less. *Gut.* 2005; **54**: 1151–6.
30. Lencioni R, Allgaier HP, Cioni D, et al. Small hepatocellular carcinoma in cirrhosis: randomized comparison of radio-frequency thermal ablation versus percutaneous ethanol injection. *Radiology.* 2003; **228**: 235–40.
31. Germani G, Pleguezuelo M, Gurusamy K, et al. Clinical outcomes of radiofrequency ablation, percutaneous alcohol and acetic acid injection for hepatocellular carcinoma: a meta-analysis. *J Hepatol.* 2010; **52**: 380–8.
32. Giorgio A, Di Sarno A, De Stefano G, et al. Percutaneous radiofrequency ablation of hepatocellular carcinoma compared to percutaneous ethanol injection in treatment of cirrhotic patients: an Italian randomized controlled trial. *Anticancer Res.* 2011; **31**: 2291–5.
33. Park YK, Kim BW, Wang HJ, Kim MW. Hepatic resection for hepatocellular carcinoma meeting Milan criteria in Child-Turcotte-Pugh class a patients with cirrhosis. *Transplant Proc.* 2009; **41**: 1691–7.
34. Wang CC, Iyer SG, Low JK, et al. Perioperative factors affecting long-term outcomes of 473 consecutive patients undergoing hepatectomy for hepatocellular carcinoma. *Ann Surg Oncol.* 2009; **16**: 1832–42.
35. Kamiyama T, Nakanishi K, Yokoo H, et al. Recurrence patterns after hepatectomy of hepatocellular carcinoma: implication of Milan criteria utilization. *Ann Surg Oncol.* 2009; **16**: 1560–71.
36. Yamamoto J, Kosuge T, Saiura A, et al. Effectiveness of hepatic resection for early-stage hepatocellular carcinoma in cirrhotic patients: subgroup analysis according to Milan criteria. *Jpn J Clin Oncol.* 2007; **37**: 287–95.
37. Nuzzo G, Giuliante F, Gauzolino R, et al. Liver resections for hepatocellular carcinoma in chronic liver disease: experience in an Italian centre. *Eur J Surg Oncol.* 2007; **33**: 1014–8.
38. Hanazaki K, Kajikawa S, Shimozaawa N, et al. Survival and recurrence after hepatic resection of 386 consecutive patients with hepatocellular carcinoma. *J Am Coll Surg.* 2000; **191**: 381–8.
39. Shimada K, Sano T, Sakamoto Y, Kosuge T. A long-term follow-up and management study of hepatocellular carcinoma patients surviving for 10 years or longer after curative hepatectomy. *Cancer.* 2005; **104**: 1939–47.
40. Huang GT, Lee PH, Tsang YM, et al. Percutaneous ethanol injection versus surgical resection for the treatment of small hepatocellular carcinoma: a prospective study. *Ann Surg.* 2005; **242**: 36–42.
41. Castells A, Bruix J, Bru C, et al. Treatment of small hepatocellular carcinoma in cirrhotic patients: a cohort study comparing surgical resection and percutaneous ethanol injection. *Hepatology.* 1993; **18**: 1121–6.
42. Livraghi T, Bolondi L, Buscarini L, et al. No treatment, resection and ethanol injection in hepatocellular carcinoma: a retrospective analysis of survival in 391 patients with cirrhosis. Italian Cooperative HCC Study Group. *J Hepatol.* 1995; **22**: 522–6.
43. Ryu M, Shimamura Y, Kinoshita T, et al. Therapeutic results of resection, transcatheter arterial embolization and percutaneous transhepatic ethanol injection in 3225 patients with hepatocellular carcinoma: a retrospective multicenter study. *Jpn J Clin Oncol.* 1997; **27**: 251–7.
44. Arii S, Yamaoka Y, Futagawa S, et al. Results of surgical and nonsurgical treatment for small-sized hepatocellular carcinomas: a retrospective and nationwide survey in Japan. The liver cancer study group of Japan. *Hepatology.* 2000; **32**: 1224–9.

Soluble MICA and a *MICA* Variation as Possible Prognostic Biomarkers for HBV-Induced Hepatocellular Carcinoma

Vinod Kumar^{1,2*}, Paulisally Hau Yi Lo¹, Hiromi Sawai³, Naoya Kato⁴, Atsushi Takahashi², Zhenzhong Deng¹, Yuji Urabe¹, Hamdi Mbarek¹, Katsushi Tokunaga³, Yasuhito Tanaka⁵, Masaya Sugiyama⁶, Masashi Mizokami⁶, Ryosuke Muroyama⁴, Ryosuke Tateishi⁷, Masao Omata⁷, Kazuhiko Koike⁷, Chizu Tanikawa¹, Naoyuki Kamatani², Michiaki Kubo², Yusuke Nakamura¹, Koichi Matsuda¹

1 Laboratory of Molecular Medicine, Human Genome Center, Institute of Medical Science, The University of Tokyo, Tokyo, Japan, **2** Center for Genomic Medicine, The Institute of Physical and Chemical Research (RIKEN), Kanagawa, Japan, **3** Department of Human Genetics, Graduate School of Medicine, The University of Tokyo, Tokyo, Japan, **4** Unit of Disease Control Genome Medicine, The Institute of Medical Science, The University of Tokyo, Tokyo, Japan, **5** Department of Clinical Molecular Informative Medicine, Nagoya City University Graduate School of Medical Sciences, Aichi, Japan, **6** The Research Center for Hepatitis and Immunology, National Center for Global Health and Medicine, Chiba, Japan, **7** Department of Gastroenterology, Graduate School of Medicine, The University of Tokyo, Tokyo, Japan

Abstract

MHC class I polypeptide-related chain A (MICA) molecule is induced in response to viral infection and various types of stress. We recently reported that a single nucleotide polymorphism (SNP) rs2596542 located in the *MICA* promoter region was significantly associated with the risk for hepatitis C virus (HCV)-induced hepatocellular carcinoma (HCC) and also with serum levels of soluble MICA (sMICA). In this study, we focused on the possible involvement of MICA in liver carcinogenesis related to hepatitis B virus (HBV) infection and examined correlation between the *MICA* polymorphism and the serum sMICA levels in HBV-induced HCC patients. The genetic association analysis revealed a nominal association with an SNP rs2596542; a G allele was considered to increase the risk of HBV-induced HCC ($P=0.029$ with odds ratio of 1.19). We also found a significant elevation of sMICA in HBV-induced HCC cases. Moreover, a G allele of SNP rs2596542 was significantly associated with increased sMICA levels ($P=0.009$). Interestingly, HCC patients with the high serum level of sMICA (>5 pg/ml) exhibited poorer prognosis than those with the low serum level of sMICA (≤ 5 pg/ml) ($P=0.008$). Thus, our results highlight the importance of *MICA* genetic variations and the significance of sMICA as a predictive biomarker for HBV-induced HCC.

Citation: Kumar V, Yi Lo PH, Sawai H, Kato N, Takahashi A, et al. (2012) Soluble MICA and a *MICA* Variation as Possible Prognostic Biomarkers for HBV-Induced Hepatocellular Carcinoma. PLoS ONE 7(9): e44743. doi:10.1371/journal.pone.0044743

Editor: Erica Villa, University of Modena & Reggio Emilia, Italy

Received: May 3, 2012; **Accepted:** August 7, 2012; **Published:** September 14, 2012

Copyright: © 2012 Kumar et al. This is an open-access article distributed under the terms of the Creative Commons Attribution License, which permits unrestricted use, distribution, and reproduction in any medium, provided the original author and source are credited.

Funding: This work was conducted as a part of the BioBank Japan Project that was supported by the Ministry of Education, Culture, Sports, Science and Technology of the Japanese government. The funders had no role in study design, data collection and analysis, decision to publish, or preparation of the manuscript.

Competing Interests: The authors have declared that no competing interests exist.

* E-mail: koichima@ims.u-tokyo.ac.jp

Introduction

Hepatocellular carcinoma (HCC) reveals a very high mortality rate that is ranked the third among all cancers in the world [1]. HCC is known to develop in a multistep process which has been related to various risk factors such as genetic factors, environment toxins, alcohol and drug abuse, autoimmune disorders, elevated hepatic iron levels, obesity, and hepatotropic viral infections [2]. Among them, chronic infection with hepatitis B virus (HBV) is one of the major etiological factors for developing HCC with considerable regional variations ranging from 20% of HCC cases in Japan to 65% in China [3].

Interestingly, clinical outcome after the exposure to HBV considerably varies between individuals. The great majority of individuals infected with HBV spontaneously eliminate the viruses, but a subset of patients show the persistent chronic hepatitis B infection (CHB), and then progresses to liver cirrhosis and HCC through a complex interplay between multiple genetic and

environmental factors [4]. In this regard, genome wide association studies (GWAS) using single nucleotide polymorphisms (SNPs) have highlighted the importance of genetic factors in the pathogenesis of various diseases including CHB as well as HBV-induced HCC [5,6,7,8,9,10,11,12,13]. Recently, we identified a genetic variant located at 4.7 kb upstream of the *MHC class I polypeptide-related chain A (MICA)* gene to be strongly associated with hepatitis C virus (HCV)-induced HCC development [14].

MICA is highly expressed on viral-infected cells or cancer cells, and acts as ligand for NKG2D to activate antitumor effects of Natural killer (NK) cells and CD8⁺ T cells [15,16]. Our previous results indicated that a G allele of SNP rs2596542 was significantly associated with the lower cancer risk and the higher level of soluble MICA (sMICA) in the serum of HCV-induced HCC patients, demonstrating the possible role of MICA as a tumor suppressor. However, elevation of serum sMICA was shown to be associated with poor prognosis in various cancer patients [17,18,19,20].

Matrix metalloproteinases (MMPs) can cleave MICA at a transmembrane domain [21] and release sMICA proteins from cells. Since sMICA was shown to inhibit the antitumor effects of NK cells and CD8⁺ T cells by reduction of their affinity to binding to target cells [22,23], the effect of MICA in cancer cells would be modulated by the expression of MMPs. To elucidate the role of MICA in HBV-induced hepatocellular carcinogenesis, we here report analysis of the *MICA* polymorphism and serum sMICA level in HBV-induced HCC cases.

Materials and Methods

Study participants

The demographic details of study participants are summarized in Table 1. A total of 181 HCC cases, 597 CHB patients, and 4,549 non-HBV controls were obtained from BioBank Japan that was initiated in 2003 with the funding from the Ministry of Education, Culture, Sports, Science and Technology, Japan [24]. In the Biobank Japan Project, DNA and serum of patients with 47 diseases were collected through collaborating network of 66 hospitals throughout Japan. List of participating hospitals is shown in the following website (http://biobankjp.org/plan/member_hospital.html). A total of 226 HCC cases, 102 CHB patients, and 174 healthy controls were additionally obtained from the University of Tokyo. The diagnosis of chronic hepatitis B was conducted on the basis of HBsAg-seropositivity and elevated serum aminotransferase levels for more than six months according to the guideline for diagnosis and treatment of chronic hepatitis (The Japan Society of Hepatology, <http://www.jsh.or.jp/medical/gudelines/index.html>). Control Japanese DNA samples (n=934) were obtained from Osaka-Midosuji Rotary Club, Osaka, Japan. All HCC patients were histopathologically diagnosed. Overall survival was defined as the time from blood sampling for sMICA test to the date of death due to HCC. Patients who were alive on the date of last follow-up were censored on that date. All participants provided written informed consent. This research project was approved by the ethics committee of the University of Tokyo and the ethics committee of RIKEN. All clinical assessments and specimen collections were conducted according to Declaration of Helsinki principles.

SNP genotyping

Genotyping platforms used in this study were shown in Table 1. We genotyped 181 HCC cases and 5,483 non-HBV control samples using either Illumina Human Hap610-Quad or Human Hap550v3. The other samples were genotyped at SNP rs2596542

by the Invader assay system (Third Wave Technologies, Madison, WI).

MICA variable number tandem repeat (VNTR) locus genotyping

Genotyping of the *MICA* VNTR locus in 176 HBV-induced HCC samples was performed using the primers reported previously by the method recommended by Applied Biosystems (Foster City, CA) [14]. Briefly, the 5' end of forward primer was labeled with 6-FAM, and reverse primer was modified with GTGTCTT non-random sequence at the 5' end to promote Plus A addition. The PCR products were mixed with Hi-Di Formamide and GeneScan-600 LIZ size standard, and separated by GeneScan system on a 3730x1 DNA analyzer (Applied Biosystems, Foster City, CA). GeneMapper software (Applied Biosystems, Foster City, CA) was employed to assign the repeat fragment size (Figure S1).

Quantification of soluble MICA

We obtained serum samples of 111 HBV-positive HCC samples, 129 HCV-positive HCC samples, and 60 non-HBV controls from Biobank Japan. Soluble MICA levels were measured by sandwich enzyme-linked immunosorbent assay, as described in the manufacturer's instructions (R&D Systems, Minneapolis, MN).

Statistical analysis

The association between a SNP rs2596542 and HBV-induced HCC was tested by Cochran-Armitage trend test. The Odds ratios were calculated by considering a major allele as a reference. Statistical comparisons between genotypes and sMICA levels were performed by Kruskal-Wallis test (if more than two classes for comparison) or Wilcoxon rank test using R. Overall survival rate of the patients was analyzed by Kaplan-Meier method in combination with log-rank test with SPSS 20 software. The period for the survival analysis was calculated from the date of blood sampling to the recorded date of death or the last follow-up date. Differences with a P value of <0.05 were considered statistically significant.

Results

Association of SNP rs2596542 with HBV-induced HCC

In order to examine the effect of rs2596542 genotypes on the susceptibility to HBV-induced HCC, a total of 407 HCC cases and 5,657 healthy controls were genotyped. The Cochran Armitage trend test of the data revealed a nominal association

Table 1. Demographic details of subjects analyzed.

Subjects	Source	Genotyping platform	Number of Sample	Female (%)	Age (mean+/-sd)
Liver Cancer	BioBank Japan	Illumina Human Hap610-Quad	181	17.9	62.94±9.42
	University of Tokyo	Invader assay	226		
Control	BioBank Japan	Illumina Human Hap550v3	4549	47.95	55.19±12.5
	Osaka**	Illumina Human Hap550v3	934		
	University of Tokyo	Invader assay	174		
Chronic hepatitis B*	BioBank Japan	Invader assay	597	45.66	61.31±12.6
	University of Tokyo	Invader assay	102		

*Chronic hepatitis B patients without liver cirrhosis and liver cancer during enrollment.

**Healthy volunteers from Osaka Midosuji Rotary Club, Osaka, Japan.

doi:10.1371/journal.pone.0044743.t001

between HBV-induced HCC and rs2596542 in which a risk allele G was more frequent among HBV-induced HCC cases than an A allele ($P=0.029$, OR = 1.19, 95% CI: 1.02–1.4; Table 2). To further investigate the effect of rs2596542 on the progression from CHB to HBV-induced HCC, we genotyped a total of 699 CHB cases without HCC. Although the progression risk from CHB to HBV-induced HCC was not statistically significant with rs2596542 ($P=0.197$ by the Cochran Armitage trend test with an allelic OR = 1.3 (0.94–1.36); Table 2), we found a similar trend of association in which the frequency of a risk-allele G was higher among HBV-induced HCC patients than that of CHB subjects. Since we previously revealed that an A allele was associated with a higher risk of HCV-induced HCC with OR of 1.36 [14], the rs2596542 alleles that increased the risk of HCC were opposite in HBV-induced HCC and HCV-induced HCC.

Soluble MICA levels are associated with SNP rs2596542

We subsequently performed measurement of soluble MICA (sMICA) in serum samples using the ELISA method in 176 HBV-positive HCC cases and 60 non-HBV controls. Nearly 30% of the HBV-induced HCC cases revealed the serum sMICA level of >5 pg/ml (defined as high) while the all control individuals except one showed that of ≤ 5 pg/ml (defined as low) ($P=4.5 \times 10^{-6}$; Figure 1A). Then, we examined correlation between SNP rs2596542 genotypes and serum sMICA levels in HBV-positive HCC cases. Interestingly, rs2596542 genotypes were significantly associated with serum sMICA levels ($P=0.009$; Figure 1B); 39% of individuals with the GG genotype and 20% of those with the AG genotype were classified as high for serum sMICA, but only 11% of those with the AA genotype were classified as high (AA+AG vs GG; $P=0.003$) (Figure 1B). These findings were similar with our previous reports in which a G allele was associated with higher serum sMICA levels in HCV-induced HCC patients [14].

Negative association of variable number of tandem repeat (VNTR) with sMICA level

The *MICA* gene harbors a VNTR locus in exon 5 that consists of 4, 5, 6, or 9 repeats of GCT as well as a G nucleotide insertion into a five-repeat allele (referred as A4, A5, A6, A9, and A5.1, respectively). The insertion of G (A5.1) causes a premature translation termination and results in loss of a transmembrane domain, which may produce the shorter form of the MICA protein that is likely be secreted into serum [25]. However, the association of this VNTR locus with serum sMICA level was controversial among studies [14,26,27,28]. Therefore, we examined the association between the VNTR locus and sMICA level in HBV-induced HCC patients, and found no significant association (Figure S1 and S2), concordant with our previous report for HCV-induced HCC patients [14].

Soluble MICA levels are associated with survival of HCC patients

In order to evaluate the prognostic significance of serum sMICA levels in HCC patients, we performed survival analysis of HCC patients. A total of 111 HBV-infected HCC patients and 129 HCV-infected HCC patients were included in this analysis. The mean survival period for HBV- and HCV-infected patients with less than 5 pg/ml of serum sMICA were 67.1 months (95% CI: 61.1–73.1, $n=83$), and 58.2 months (95% CI: 51.4–65.0, $n=85$), respectively. On the other hand, for patients with more than 5 pg/ml of serum sMICA, the mean survival periods were 47.8 months (95% CI: 34.8–30.9, $n=28$) for HBV-induced HCC patients and 59.5 months (95% CI: 51.9–67.1, $n=44$) for HCV-induced HCC patients. The Kaplan-Meier analysis and log-rank test indicated that among HBV-induced HCC subjects, the patients in the high serum sMICA group showed a significantly shorter survival than those in the low serum sMICA ($P=0.008$; Figure 2). In addition, we performed multi-variate analysis to test whether sMICA is an independent prognostic factor by including age and gender as covariates. The results revealed significant association of sMICA levels with overall survival ($P=0.017$) but not with age and gender (Table S1). However, we found no association between the serum sMICA level and the overall survival in the HCV-induced HCC subjects ($P=0.414$; Figure S3). Taken together, our findings imply the distinct roles of the *MICA* variation and sMICA between HBV- and HCV-induced hepatocellular carcinogenesis.

Vascular invasion in HBV-related HCC patients is associated with soluble MICA levels

Since sMICA levels were associated with the overall survival of HBV-related HCC patients, we tested whether sMICA levels affect survival through modulating invasive properties of tumors or size of the tumors. We tested the association between sMICA levels and vascular invasion in 35 HBV-related HCC cases, among whom 7 cases were positive and 21 cases were negative for vascular invasion. We found significant association between sMICA levels and vascular invasion (Figure 3; $P=0.014$) in which 7 cases with positive vascular invasion showed high levels of sMICA (mean = 54 pg/ml) than 21 cases without vascular invasion (mean = 7.51 pg/ml). However, we found no association between tumor size and sMICA levels ($P=0.56$; data not shown). These results suggest that sMICA may reduce the survival of HBV-related HCC patients by affecting the invasive properties of tumors.

Discussion

Several mechanisms such as HBV-genome integration into host chromosomal DNA [29] and effects of viral proteins including HBx [30] are shown to contribute to development and progression of HCC, while the immune cells such as NK and T cells function as key antiviral and antitumor effectors. MICA protein has been

Table 2. Association between HCC and rs2596542.

SNP	Comparison	Chr	Locus	Case MAF	Control MAF	P^*	OR*	95% CI
rs2596542	HCC vs. Healthy control	6	<i>MICA</i>	0.294	0.332	0.029	1.19	1.02–1.4
rs2596542	HCC vs. CHB	6	<i>MICA</i>	0.294	0.320	0.197	1.13	0.94–1.36

Note: 407 HCC cases, 699 CHB subjects and 5,657 non-HBV controls were used in the analysis. Chr., chromosome; MAF, minor allele frequency; OR, odds ratio for minor allele; CI, confidence interval.

*Obtained by Armitage trend test.
doi:10.1371/journal.pone.0044743.t002

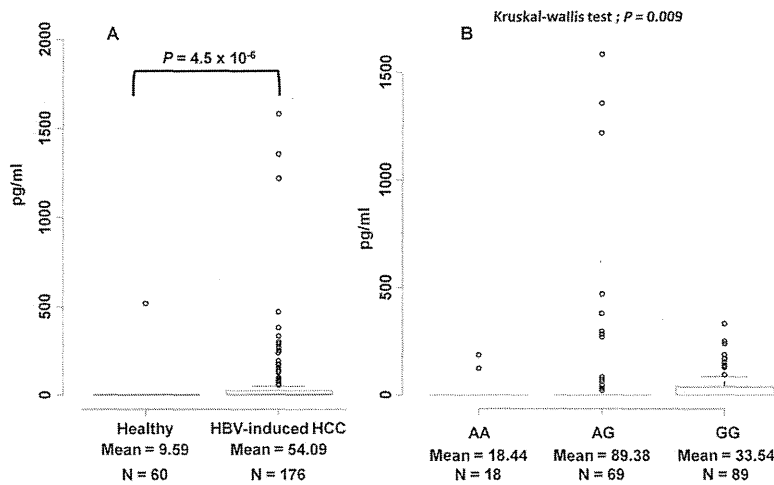


Figure 1. Soluble MICA levels are associated with HBV-related HCC. (A) Correlation between soluble MICA levels and HBV-induced HCC subjects. The y-axis displays the concentration of soluble MICA in pg/ml. The number of independent samples tested in each group is shown in the x-axis. Each group is shown as a box plot and the mean values are shown in the x-axis. The difference between two groups is tested by Wilcoxon rank test. The box plots are plotted using default settings in R. (B) Correlation between soluble MICA levels and rs2596542 genotype in HBV-positive HCC subjects. The x-axis shows the genotypes at rs2596542 and y-axis display the concentration of soluble MICA in pg/ml. Each group is shown as a box plot. $P = 0.027$ and 0.013 for AA vs. GG and AA vs. AG, respectively. The association between genotypes and sMICA levels was tested by Kruskal-wallis test, whereas the difference in the sMICA levels between AA and GG is tested by Wilcoxon rank test. The box plots are plotted using default settings in R.

doi:10.1371/journal.pone.0044743.g001

considered as a stress marker of gastrointestinal epithelial cells because of its induced expression by several external stimuli such as heat, DNA damage, and viral infections [31,32,33,34]. Here,

we examined the association of rs2596542 and serum sMICA levels with HBV-induced HCC. Like in HCV-induced HCC [14], our results from ELISA revealed a significantly higher proportion

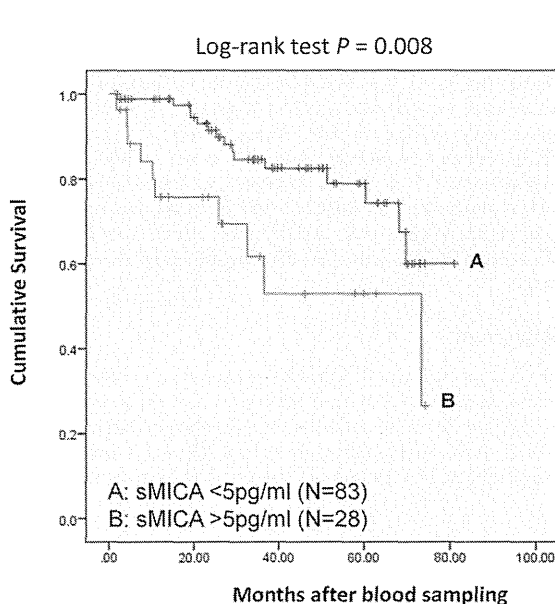


Figure 2. Kaplan-Meier curves of the patients with HBV-induced HCC. The patients were divided into two groups according to their sMICA concentration (high: >5 pg/ml and low: ≤ 5 pg/ml). Statistical difference was analyzed by log-rank test. The y-axis shows the cumulative survival probability and x-axis display the months of the patient's survival after blood sampling. doi:10.1371/journal.pone.0044743.g002

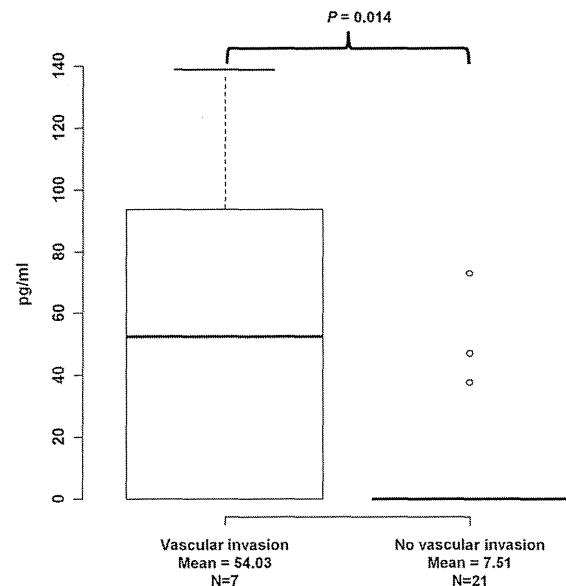


Figure 3. Correlation between soluble MICA levels and vascular invasion in HBV-induced HCC subjects. The y-axis displays the concentration of soluble MICA in pg/ml. The number of independent samples tested in each group is shown in the x-axis. Each group is shown as a box plot and the mean values are shown in the x-axis. The difference between two groups is tested by Wilcoxon rank test. The box plots are plotted using default settings in R. doi:10.1371/journal.pone.0044743.g003

of high serum sMICA cases (nearly 30%) in the HBV-induced HCC group, compared to non-HBV individuals (1.7%). Moreover, the serum sMICA level was significantly associated with rs2596542, but not with the copy number differences of the VNTR locus, as concordant with our previous report [14].

Several studies have already indicated the roles of sMICA as prognostic markers for different types of malignant diseases [17,18,19,20]. Therefore, it is of medical importance to test whether serum sMICA levels can be used as a prognostic marker for patients with HCC. To our best knowledge, this is the first study to demonstrate the prognostic potential of sMICA for HBV-positive HCC patients; we found 19.3 months of improvement in survival among patients carrying less than 5 pg/ml of serum sMICA, compared to those having more than 5 pg/ml.

On the contrary, we found no significant correlation between sMICA levels and the prognosis of HCV-induced HCC cases. These opposite effects of *MICA* variation could be explained by the following mechanism. The individuals who carry the G allele would express high levels of membrane-bound MICA upon HCV infection and thus lead to the activation of immune cells against virus infected cells. On one hand, HBV infection results in increased expression of membrane-bound MICA as well as MMPs through viral protein HBx [35], which would result in the elevation of sMICA and the reduction of membrane-bound MICA. Since sMICA could block CD8+T cells, NK-CTL, and NK cells, higher sMICA would cause the inactivation of immune surveillance system against HBV infected cells. In other words, HBV may use this strategy to evade immune response and hence, higher levels of sMICA could be associated with lower survival rate among HBV-associated HCC. On the other hand, since HCV is not known to induce the cleavage of membrane bound MICA, individuals with low level membrane bound MICA expression (carriers of rs2596542-allele A) could be inherently susceptible for HCV-induced HCC. Thus, HBx-mediated induction of MMPs could partially explain the intriguing contradictory effect of MICA between HBV-induced HCC and HCV-induced HCC. Since we observed significant correlation of sMICA levels with vascular invasion, it may be the case that high levels of sMICA cause poor prognosis of HBV-related HCC cases by making tumors more aggressive and invasive. However it is important in future to determine the ratio of membrane-bound MICA to sMICA in case of HCV- and HBV-related HCC.

Interestingly, the immune therapy against melanoma patients induced the production of auto-antibodies against MICA [36]. Anti-MICA antibodies would exert antitumor effects through antibody-dependent cellular cytotoxicity against cells expressing membrane-bound MICA and/or activation of NK cells by inhibiting the sMICA-NKG2D interaction. However, further studies are necessary, using well-defined HBV-related HCC

cohort, to investigate whether sMICA levels could be included as an additional factor to predict the survival rate among HBV-related HCC subjects. Taken together, our results indicate the potential of *MICA* variant and sMICA as prognostic biomarkers. Thus, MICA could be a useful therapeutic target for HBV-induced HCC.

Supporting Information

Figure S1 MICA repeat genotyping using capillary-based method. The alleles are annotated using GeneMapper software based on the size of the PCR product (185 bp = A4 allele, 188 bp = A5, 189 bp = A5.1, 191 bp = A6 and 200 bp = A9). The inset at the base of each peak shows the size of the PCR product with corresponding allele call by the software. The figure display all observed heterozygotes at A5.1 allele.

(TIF)

Figure S2 MICA VNTR alleles are not associated with soluble MICA levels. Each group is shown as a box plot. The difference in the sMICA values among each group is tested by Wilcoxon rank test. The box plots are plotted using default settings in R.

(TIF)

Figure S3 Kaplan-Meier curves of the patients with HCV-induced HCC. The patients were divided into two groups according to their sMICA concentration (<5 pg/ml or >5 pg/ml). Statistical difference was analyzed by log-rank test. The y-axis shows the cumulative survival probability and x-axis display the months of the patients survival after blood sampling.

(TIF)

Table S1 Clinical parameters of HBV-related HCC patients available for prognostic analyses.

(XLS)

Acknowledgments

We would like to thank all the patients and the members of the Rotary Club of Osaka-Midosuji District 2660 Rotary International in Japan, who donated their DNA for this work. We also thank Ayako Matsui and Hiroe Tagaya (the University of Tokyo), and the technical staff of the Laboratory for Genotyping Development, Center for Genomic Medicine, RIKEN for their technical support.

Author Contributions

Conceived and designed the experiments: VK KM YN. Performed the experiments: VK PHL YU HM ZD. Analyzed the data: VK PHL CT RM. Contributed reagents/materials/analysis tools: YN NK AT MK HS KT YT MS MM RT MO KK NK. Wrote the paper: VK PHL KM YN.

References

1. Kew MC (2010) Epidemiology of chronic hepatitis B virus infection, hepatocellular carcinoma, and hepatitis B virus-induced hepatocellular carcinoma. *Pathol Biol (Paris)* 58: 273–277.
2. Sherman M (2010) Hepatocellular carcinoma: epidemiology, surveillance, and diagnosis. *Semin Liver Dis* 30: 3–16.
3. Perz J, Armstrong G, Farrington L, Hutin Y, Bell B (2006) The contributions of hepatitis B virus and hepatitis C virus infections to cirrhosis and primary liver cancer worldwide. *J Hepatol* 45: 529–538.
4. Chen CJ, Chen DS (2002) Interaction of hepatitis B virus, chemical carcinogen, and genetic susceptibility: multistage hepatocarcinogenesis with multifactorial etiology. *Hepatology* 36: 1046–1049.
5. Cui R, Okada Y, Jang SG, Ku JL, Park JG, et al. (2011) Common variant in 6q26–q27 is associated with distal colon cancer in an Asian population. *Gut* 60: 799–805.
6. Kumar V, Matsuo K, Takahashi A, Hosono N, Tsunoda T, et al. (2011) Common variants on 14q32 and 13q12 are associated with DLBCL susceptibility. *J Hum Genet England*. pp. 436–439.
7. Cui R, Kamatani Y, Takahashi A, Usami M, Hosono N, et al. (2009) Functional variants in ADH1B and ALDH2 coupled with alcohol and smoking synergistically enhance esophageal cancer risk. *Gastroenterology* 137: 1768–1775.
8. Urabe Y, Tanikawa C, Takahashi A, Okada Y, Morizono T, et al. (2012) A genome-wide association study of nephrolithiasis in the Japanese population identifies novel susceptible loci at 5q35.3, 7p14.3 and 13q14.1. *PLOS Genet* 8(3): e1002541.
9. Tanikawa C, Urabe Y, Matsuo K, Kubo M, Takahashi A, et al. (2012) A genome-wide association study identifies two susceptibility loci for duodenal ulcer in the Japanese population. *Nat Genet* 44(4): 430–434.

10. Hata J, Matsuda K, Ninomiya T, Yonemoto K, Matsushita T, et al. (2007) Functional SNP in an Sp1-binding site of AGTRL1 gene is associated with susceptibility to brain infarction. *Hum Mol Genet* 16: 630–639.
11. Kamatani Y, Wattanapokayakit S, Ochi H, Kawaguchi T, Takahashi A, et al. (2009) A genome-wide association study identifies variants in the HLA-DP locus associated with chronic hepatitis B in Asians. *Nat Genet* 41: 591–595.
12. Mbarek H, Ochi H, Urabe Y, Kumar V, Kubo M, et al. (2011) A genome-wide association study of chronic hepatitis B identified novel risk locus in a Japanese population. *Human Molecular Genetics* 20: 3884–3892.
13. Zhang H, Zhai Y, Hu Z, Wu C, Qian J, et al. (2010) Genome-wide association study identifies 1p36.22 as a new susceptibility locus for hepatocellular carcinoma in chronic hepatitis B virus carriers. *Nat Genet* 42: 755–758.
14. Kumar V, Kato N, Urabe Y, Takahashi A, Muroyama R, et al. (2011) Genome-wide association study identifies a susceptibility locus for HCV-induced hepatocellular carcinoma. *Nature genetics* 43: 455–458.
15. Jinushi M, Takehara T, Tatsumi T, Kanto T, Groh V, et al. (2003) Expression and role of MICA and MICB in human hepatocellular carcinomas and their regulation by retinoic acid. *Int J Cancer* 104: 354–361.
16. Bauer S, Groh V, Wu J, Steinle A, Phillips JH, et al. (1999) Activation of NK cells and T cells by NKG2D, a receptor for stress-inducible MICA. *Science* 285: 727–729.
17. Holdenrieder S, Stieber P, Peterfi A, Nagel D, Steinle A, et al. (2006) Soluble MICA in malignant diseases. *Int J Cancer* 118: 684–687.
18. Nüchel H, Switala M, Sellmann L, Horn PA, Dürig J, et al. (2010) The prognostic significance of soluble NKG2D ligands in B-cell chronic lymphocytic leukemia. *Leukemia* 24: 1152–1159.
19. Tamaki S, Sanefuzi N, Kawakami M, Aoki K, Imai Y, et al. (2008) Association between soluble MICA levels and disease stage IV oral squamous cell carcinoma in Japanese patients. *Hum Immunol* 69: 88–93.
20. Li K, Mandai M, Hamanishi J, Matsumura N, Suzuki A, et al. (2009) Clinical significance of the NKG2D ligands, MICA/B and ULBP2 in ovarian cancer: high expression of ULBP2 is an indicator of poor prognosis. *Cancer Immunol Immunother* 58: 641–652.
21. Salih H, Rammensee H, Steinle A (2002) Cutting edge: down-regulation of MICA on human tumors by proteolytic shedding. *J Immunol* 169: 4098–4102.
22. Groh V, Wu J, Yee C, Spies T (2002) Tumour-derived soluble MIC ligands impair expression of NKG2D and T-cell activation. *Nature* 419: 734–738.
23. Jinushi M, Takehara T, Tatsumi T, Hiramatsu N, Sakamori R, et al. (2005) Impairment of natural killer cell and dendritic cell functions by the soluble form of MHC class I-related chain A in advanced human hepatocellular carcinomas. *J Hepatol* 43: 1013–1020.
24. Nakamura Y (2007) The BioBank Japan Project. *Clin Adv Hematol Oncol* 5: 696–697.
25. Ota M, Katsuyama Y, Mizuki N, Ando H, Furihata K, et al. (1997) Trinucleotide repeat polymorphism within exon 5 of the MICA gene (MHC class I chain-related gene A): allele frequency data in the nine population groups Japanese, Northern Han, Hui, Uyghur, Kazakhstan, Iranian, Saudi Arabian, Greek and Italian. *Tissue Antigens* 49: 448–454.
26. Tamaki S, Sanefuzi N, Ohgi K, Imai Y, Kawakami M, et al. (2007) An association between the MICA-A5.1 allele and an increased susceptibility to oral squamous cell carcinoma in Japanese patients. *J Oral Pathol Med* 36: 351–356.
27. Tamaki S, Kawakami M, Yamanaka Y, Shimomura H, Imai Y, et al. (2009) Relationship between soluble MICA and the MICA A5.1 homozygous genotype in patients with oral squamous cell carcinoma. *Clin Immunol* 130: 331–337.
28. Lü M, Xia B, Ge L, Li Y, Zhao J, et al. (2009) Role of major histocompatibility complex class I-related molecules A* A5.1 allele in ulcerative colitis in Chinese patients. *Immunology* 128: e230–236.
29. Bonilla Guerrero R, Roberts LR (2005) The role of hepatitis B virus integrations in the pathogenesis of human hepatocellular carcinoma. *J Hepatol* 42: 760–777.
30. Bouchard MJ, Schneider RJ (2004) The enigmatic X gene of hepatitis B virus. *J Virol* 78: 12725–12734.
31. Groh V, Bahram S, Bauer S, Herman A, Beauchamp M, et al. (1996) Cell stress-regulated human major histocompatibility complex class I gene expressed in gastrointestinal epithelium. *Proc Natl Acad Sci U S A* 93: 12445–12450.
32. Groh V, Steinle A, Bauer S, Spies T (1998) Recognition of stress-induced MHC molecules by intestinal epithelial gammadelta T cells. *Science* 279: 1737–1740.
33. Groh V, Rhinehart R, Randolph-Habecker J, Topp M, Riddell S, et al. (2001) Costimulation of CD8alphabeta T cells by NKG2D via engagement by MIC induced on virus-infected cells. *Nat Immunol* 2: 255–260.
34. Gasser S, Orsulic S, Brown EJ, Raulet DH (2005) The DNA damage pathway regulates innate immune system ligands of the NKG2D receptor. *Nature* 436: 1186–1190.
35. Lara-Pezzi E, Gomez-Gavero MV, Galvez BG, Mira E, Iniguez MA, et al. (2002) The hepatitis B virus X protein promotes tumor cell invasion by inducing membrane-type matrix metalloproteinase-1 and cyclooxygenase-2 expression. *J Clin Invest* 110: 1831–1838.
36. Jinushi M, Hodi F, Dranoff G (2006) Therapy-induced antibodies to MHC class I chain-related protein A antagonize immune suppression and stimulate antitumor cytotoxicity. *Proc Natl Acad Sci U S A* 103: 9190–9195.

A genome-wide association study of HCV-induced liver cirrhosis in the Japanese population identifies novel susceptibility loci at the MHC region

Yuji Urabe^{1,2}, Hidenori Ochi², Naoya Kato⁴, Vinod Kumar^{1,3}, Atsushi Takahashi³, Ryosuke Muroyama⁴, Naoya Hosono³, Motoyuki Otsuka⁵, Ryosuke Tateishi⁵, Paulisally Hau Yi Lo¹, Chizu Tanikawa¹, Masao Omata⁵, Kazuhiko Koike⁵, Daiki Miki², Hiromi Abe², Naoyuki Kamatani³, Joji Toyota⁶, Hiromitsu Kumada⁷, Michiaki Kubo³, Kazuaki Chayama², Yusuke Nakamura^{1,3}, Koichi Matsuda^{1,*}

¹Laboratory of Molecular Medicine, Human Genome Center, Institute of Medical Science, The University of Tokyo, Tokyo, Japan; ²Department of Medical and Molecular Science, Division of Frontier Medical Science, Programs for Biomedical Research, Graduate School of Biomedical Sciences, Hiroshima University, Hiroshima, Japan; ³Center for Genomic Medicine, The Institute of Physical and Chemical Research (RIKEN), Kanagawa, Japan; ⁴Unit of Disease Control Genome Medicine, The Institute of Medical Science, The University of Tokyo, Tokyo, Japan; ⁵Department of Gastroenterology, Graduate School of Medicine, The University of Tokyo, Tokyo, Japan; ⁶Department of Gastroenterology, Sapporo Kosei General Hospital, Hokkaido, Japan; ⁷Department of Hepatology, Toranomon Hospital, Tokyo, Japan

Background & Aims: We performed a genome-wide association study (GWAS) of hepatitis C virus (HCV)-induced liver cirrhosis (LC) to identify predictive biomarkers for the risk of LC in patients with chronic hepatitis C (CHC).

Methods: A total of 682 HCV-induced LC cases and 1045 CHC patients of Japanese origin were genotyped by Illumina Human Hap 610-Quad bead Chip.

Results: Eight SNPs which showed possible associations ($p < 1.0 \times 10^{-5}$) at the GWAS stage were further genotyped using 936 LC cases and 3809 CHC patients. We found that two SNPs within the major histocompatibility complex (MHC) region on chromosome 6p21, rs910049 and rs3135363, were significantly associated with the progression from CHC to LC ($p_{\text{combined}} = 9.15 \times 10^{-11}$ and 1.45×10^{-10} , odds ratio (OR) = 1.46 and 1.37, respectively). We also found that *HLA-DQA1*0601* and *HLA-DRB1*0405* were associated with the progression from CHC to LC ($p = 4.53 \times 10^{-4}$ and 1.54×10^{-4} with OR = 2.80 and 1.45, respectively). Multiple logistic regression analysis revealed that rs3135363, rs910049, and *HLA-DQA1*0601* were independently associated with the risk of HCV-induced LC. In addition, individ-

uals with four or more risk alleles for these three loci have a 2.83-fold higher risk for LC than those with no risk allele, indicating the cumulative effects of these variations.

Conclusions: Our findings elucidated the crucial roles of multiple genetic variations within the MHC region as prognostic/predictive biomarkers for CHC patients.

© 2013 European Association for the Study of the Liver. Published by Elsevier B.V. All rights reserved.

Introduction

Two million people in Japan and 210 million people worldwide are estimated to be infected with the hepatitis C virus (HCV), which is known to be a major cause of chronic viral liver disease [1]. Patients with chronic hepatitis C (CHC) usually exhibit mild inflammatory symptoms, but are at a significantly high risk for developing liver cirrhosis (LC) and hepatocellular carcinoma [2]. More than 400,000 people at present suffer from LC, which is ranked as the 9th major cause of death in Japan. In addition, liver cancer causes approximately 32,000 deaths per year, making it the 4th most common cause of death from malignant diseases. Thus, HCV-related diseases are important public health problems [3].

Clinical outcomes after the exposure to HCV vary enormously among individuals. Approximately 70% of infected persons will develop chronic hepatitis [4], and about 20–30% of CHC patients will develop cirrhosis, but others can remain asymptomatic for decades [2]. The annual death rate of patients with decompensated cirrhosis is as high as 15–30% [5]. Moreover, more than 7% of LC patients develop hepatocellular cancer in Japan and Taiwan, while the frequencies are less than 1.6% among other ethnic groups [6,7]. These inter-individual and inter-ethnic differences have been attributed to various factors such as viral genotypes,

Keywords: Genome-wide association study; Hepatitis C virus; Liver cirrhosis; Major histocompatibility complex.

Received 22 April 2012; received in revised form 15 December 2012; accepted 24 December 2012; available online 12 January 2013

* Corresponding author. Address: Laboratory of Molecular Medicine, Institute of Medical Science, The University of Tokyo, 4-6-1 Shirokanedai, Minato, Tokyo 108-8639, Japan. Tel.: +81 3 5449 5376; fax: +81 3 5449 5123.

E-mail address: koichima@ims.u-tokyo.ac.jp (K. Matsuda).

Abbreviations: CHC, chronic hepatitis C; GWAS, genome-wide association study; HCV, hepatitis C virus; LC, liver cirrhosis; MHC, major histocompatibility complex; OR, odds ratio; PBC, primary biliary cirrhosis; SNPs, single nucleotide polymorphisms.



Research Article

Table 1. Characteristics of samples and methods used in this study.

Stage	Source	Platform	Number of samples	Female (%)	Age, yr (mean \pm SD)
GWAS					
Liver cirrhosis	BioBank Japan	Illumina Human Hap 610	682	313 (46.3)	67.1 \pm 9.7
Chronic hepatitis C ^a	Hiroshima University	Illumina Human Hap 610	1045	371 (35.5)	55.2 \pm 11.0
Replication					
Liver cirrhosis	Tokyo University	Invader assay	716	334 (46.8)	64.4 \pm 10.4
	Hiroshima University		220	98 (44.5)	64.7 \pm 8.98
Chronic hepatitis C ^a	BioBank Japan	Invader assay	1670	780 (46.8)	59.7 \pm 12.6
	Hiroshima University		2139	1061 (51.8)	58.8 \pm 9.20

^aNumber of samples that qualified. CHC patients with severe liver fibrosis (F3 or F4) or lower platelet counts (<160,000) were excluded.

alcohol consumption, age at infection, co-infection of HIV or HBV [8–10], insulin resistance, steatosis, and metabolic syndrome [11]. Previous gene expression analyses also identified various genes associated with liver fibrosis among patients with CHC [12–14]. In addition, miRNAs such as mir-21 and mir-122 were shown to be correlated with liver fibrosis [15,16].

Currently, the genome-wide association study is the most common method to identify genetic variations associated with disease risk [17–20]. In addition, the roles of genetic factors in HCV-related diseases have been elucidated. *IL28B* is associated with spontaneous clearance of HCV [21] as well as with the clinical response to the combination therapy of pegylated interferon and ribavirin [22,23]. Recently, our group has shown that SNP rs2596542 on *MICA* [24] and SNP rs1012068 on *DEPDC5* [25] are significantly associated with HCV-induced liver cancer. Although liver cirrhosis is the major risk factor of liver cancer, a fraction of CHC patients will develop HCC without accompanying LC. Therefore, the underlying genetic background would be different between HCV-induced LC and HCV-induced HCC. Previous studies identified the association of genetic variants in *HLA-DQ/DR/B* [26–28], *2-5AS* [29], *TLR3* [30], and *PNPLA3* [31] with the risk of liver fibrosis among patients with CHC. However, a comprehensive approach for HCV-induced LC has not been conducted so far. Here we performed GWAS of HCV-induced LC to identify predictive biomarkers for the risk of LC in patients with CHC.

Materials and methods

Ethics statement

All subjects provided written informed consent. This project was approved by the ethical committees at University of Tokyo, Hiroshima University, Sapporo Kosei General Hospital, Toranomon Hospital, and Center for Genomic Medicine, Institutes of Physical and Chemical Research (RIKEN).

Study population

The characteristics of each cohort are shown in Table 1. In this study, we conducted GWAS and replication analysis on a total of 1618 HCV-induced LC and 4854 CHC patients. All subjects had abnormal levels of serum alanine transaminase for more than 6 months and were positive for both HCV antibody and serum HCV RNA. Among 1618 LC and 4854 CHC samples, 342 LC patients (21.14%) and 2997 CHC patients (61.70%) underwent liver biopsy. The remaining 1276 LC and 1857 CHC patients were diagnosed by non-invasive methods including hepatic imaging (e.g., ultrasonography, computed tomography, arteriography or magnetic resonance imaging), biochemical data (serum bilirubin, serum albumin, platelet, or prothrombin time), and the presence/absence of clinical manifestations of portal hypertension (e.g., varices, encephalopathy or ascites). The patients with CHC

or LC were recruited for this study regardless of their treatment history. We excluded from the analysis the followings CHC patients: (1) advanced liver fibrosis (F3 or F4 by New Inuyama classification) [32], (2) platelet count under 160,000 for patients without liver fibrosis staging, and (3) HBV co-infection. Characteristics of each study cohort are shown in Table 1. In brief, DNA of HCV-induced LC and CHC patients was obtained from Biobank Japan (<http://biobankjp.org/>) [33], the Hiroshima Liver Study Group (<http://home.hiroshima-u.ac.jp/naika1/researchprofile/pdf/liverstudygroupe.pdf>), Toranomon Hospital, and the University of Tokyo. All subjects were of Japanese origin.

SNP genotyping

Genomic DNA was extracted from peripheral blood leukocytes using a standard method. In GWAS, we genotyped 682 LC and 1045 CHC samples using Illumina Human Hap 610-Quad bead Chip (Supplementary Fig. 1). Samples with low call rate (<0.98) were excluded from our analysis (six LC and two CHC samples). We then applied SNP quality control as follows: call rate ≥ 0.99 in LC and CHC samples, Hardy–Weinberg $p \geq 1 \times 10^{-6}$ in LC and CHC samples. Consequently, 461,992 SNPs on the autosomal chromosomes passed the quality control filters. SNPs with minor allele frequency of <0.01 in both LC and CHC samples were excluded from further analyses, considering statistical power in the replication analysis. Finally, we analyzed 431,618 SNPs in GWAS. Among the top ten SNPs showing $p < 1.0 \times 10^{-5}$, we selected nine SNPs for further analysis with LD threshold of $r^2 = 0.95$. In the replication stage, we genotyped 936 LC and 3809 CHC using multiplex PCR-based Invader assay (Third Wave Technologies).

Statistical analysis

The association of SNPs with the phenotype in the GWAS, replication stage, and combined analyses was tested by logistic regression analysis, upon adjusting for age at recruitment (continuous) and gender, by assuming additive model using PLINK [34]. In the GWAS, the genetic inflation factor λ was derived by applying logistic regression p values for all the tested SNPs. The quantile–quantile plot was drawn using R program. The odds ratios were calculated using the non-susceptible allele as reference, unless stated otherwise. The combined analysis of GWAS and replication stage was verified by using the Mantel–Haenszel method. We set the significance threshold as follows; $p = 1 \times 10^{-5}$ in the GWAS stage (first stage) and $p = 6.25 \times 10^{-3}$ ($=0.05/8$) in the replication analysis. We considered $p < 5 \times 10^{-8}$ as threshold of GWAS significance in the combined analysis, which is the Bonferroni-corrected threshold for the number of independent SNPs genotyped in HapMap Phase II [35]. The heterogeneity across two stages was examined by using the Breslow–Day test [36]. We used Haploview software to analyze the association of haplotypes and LD values between SNPs. Quality control for SNPs was applied as follows: call rate ≥ 0.95 in LC and CHC samples, and Hardy–Weinberg $p \geq 1 \times 10^{-6}$ in CHC samples in replication stage. The statistical power was 19.51% in GWAS (the first stage) ($p = 1.00 \times 10^{-5}$), 97.98% in replication ($p = 0.05/8$), and 74.76% in the combined stage ($p = 5.00 \times 10^{-8}$) at minor allele frequency of 0.3 and OR of 1.3.

Imputation-based association analysis of HLA class I and class II alleles

We obtained an SNP or a combination of SNPs which could tag the HLA alleles in the Japanese population from a previous study [37]. Genotypes of tagging SNPs were imputed in the GWAS samples by using a Hidden Markov model programmed in MACH [38] and haplotype information from HapMap JPT samples

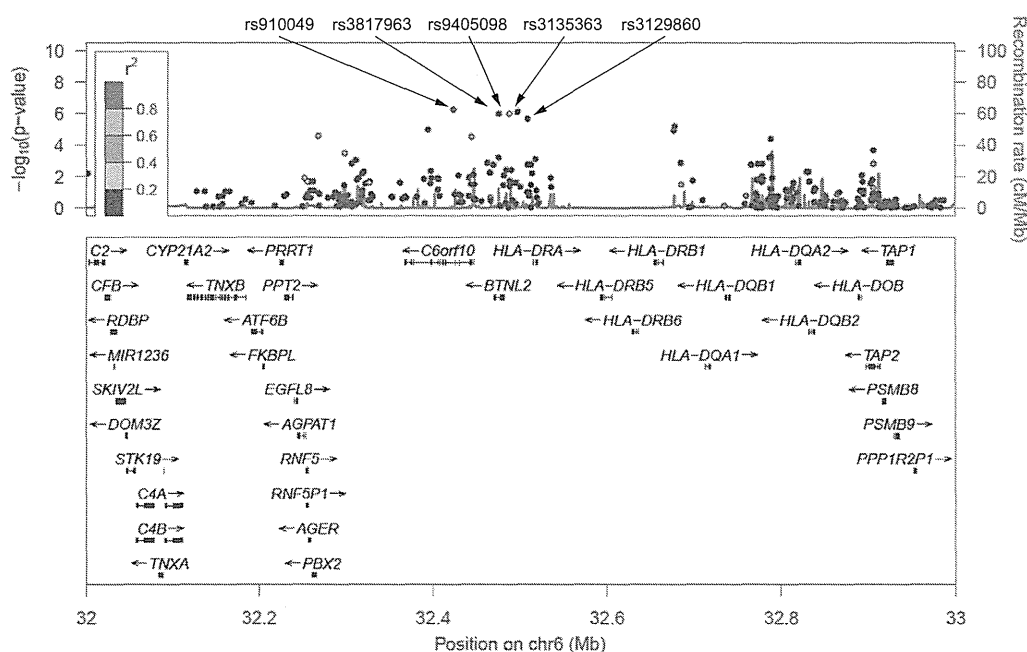


Fig. 1. Regional association plot at 6p21.3. (Upper panel) p Values of genotyped SNPs (circle) and imputed SNPs (cross) are plotted (as $-\log_{10} p$ value) against their physical position on chromosome 6 (NCBI Build 36). The p value for rs910049 at GWAS is represented by a purple diamond. Estimated recombination rates from HapMap JPT show the local LD structure. Inset; the color of the other SNPs indicates LD with rs3135363 according to a scale from $r^2 = 0$ to $r^2 = 1$ based on pair-wise r^2 values from HapMap JPT. (Lower panel) Gene annotations from the University of California Santa Cruz genome browser.

and 1000 genome imputation samples [39]. We applied the same SNP quality criteria as in GWAS, to select SNPs for the analysis. We employed the logistic regression analysis upon age and gender adjustment to assess the associations between HCV-induced LC and HLA alleles.

Software

For general statistical analysis, we employed R statistical environment version 2.9.1 (cran.r-project.org) or plink-1.06 (pngu.mgh.harvard.edu/~purcell/plink/). The Haploview software version 4.2 [40] was used to calculate LD and to draw Manhattan plot. Primer3 -web v0.3.0 (<http://frodo.wi.mit.edu>) web tool was used to design primers. We employed LocusZoom (<http://csg.sph.umich.edu/locuszoom/>) for regional plots. We used SNP Functional Prediction web tool for functional annotation of SNPs (<http://snpinfo.niehs.nih.gov/snpfunc.htm>) [41]. We used "Gene Expression Analysis Based on Imputed Genotypes" (<http://www.sph.umich.edu/csg/liang/imputation>) [42] for eQTL analysis. We used MACTH [43] web tool for searching potential binding sites for transcription factors (<http://www.gene-regulation.com/index.htm>).

Results

Genome-wide association study for HCV-induced liver cirrhosis

We performed a two-stage GWAS using a total of 1618 cases and 4854 controls (Supplementary Fig. 1). In the first stage, a whole genome scan was performed on 682 Japanese patients with HCV-induced LC and 1045 Japanese patients with CHC, using Illumina Human Hap 610-Quad bead Chip. The genotyping results of 431,618 single nucleotide polymorphisms (SNPs) obtained after our standard quality control were used for further analysis.

CHC patients with severe liver fibrosis (F3 or F4 according to the New Inuyama classification [32]) or lower platelet counts ($<160,000$) were excluded from the control group. As progression from CHC to LC is strongly affected by age and gender, we performed logistic regression analyses including age and gender as covariates at all tested loci in our analyses. The genetic inflation factor lambda was 1.051, indicating that there is little or no evidence of population stratification (Supplementary Fig. 2A). Although no SNPs cleared the GWAS significance threshold ($p < 5 \times 10^{-8}$) at the first stage, we selected ten candidate SNPs showing suggestive association of $p < 1 \times 10^{-5}$ (Supplementary Fig. 2B and Supplementary Table 1). After excluding SNP rs6891116 due to almost absolute linkage with SNP rs10252674 ($r^2 = 0.99$), the remaining nine SNPs were further genotyped using an independent cohort, consisting of 936 LC and 3809 CHC cases, by multiplex PCR-based Invader assay as the second stage. We could successfully obtain genotype results for eight SNPs after the QC filter (call rate ≥ 0.95 in LC and CHC samples, Hardy-Weinberg of $p \geq 1 \times 10^{-6}$ in CHC samples). The logistic regression analysis adjusted by age and gender revealed that five SNPs on chromosome 6q21.3 indicated a significant association with progression from CHC to LC after the Bonferroni correction ($p < 0.05/8 = 6.25 \times 10^{-3}$, Supplementary Table 2). A meta-analysis of the two stages with a fixed-effects model revealed that all of the five SNPs significantly associated with progression from CHC to LC (p values of 9.15×10^{-11} – 1.28×10^{-8} with odds ratios (OR) of 1.30–1.46, Fig. 1 and Table 2). These five SNPs were located in the HLA class II region and were in strong linkage disequilibrium with each other ($D' > 0.75$,

Research Article

Table 2. Summary of GWAS and replication analyses.

SNP	Stage	Allele (1/2)	Gene	Liver cirrhosis				Chronic hepatitis C				OR (95% CI) ^b	p value ^c	p value ^d _{het}
				11	12	22	RAF ^a	11	12	22	RAF ^a			
rs910049														
	GWAS	a/g	<i>C6orf10</i> (6p21.3)	24	217	435	0.196	25	224	794	0.131	1.73 (1.40-2.15)	5.39 × 10 ⁻⁷	
	Replication			38	259	631	0.180	66	952	2790	0.142	1.37 (1.20-1.58)	7.59 × 10 ⁻⁶	
	Combined ^e											1.46 (1.28-1.62)	9.15 × 10 ⁻¹¹	0.075
rs3817963														
	GWAS	a/g	<i>BTNL2</i> (6p21.3)	92	343	241	0.390	101	437	505	0.306	1.53 (1.29-1.81)	9.50 × 10 ⁻⁷	
	Replication			130	395	395	0.356	409	1573	1816	0.315	1.22 (1.10-1.36)	2.66 × 10 ⁻⁴	
	Combined ^e											1.30 (1.18-1.42)	1.28 × 10 ⁻⁸	0.029
rs9405098														
	GWAS	a/g	No gene (6p21.3)	75	293	308	0.328	70	365	608	0.242	1.54 (1.30-1.84)	1.10 × 10 ⁻⁶	
	Replication			100	361	462	0.304	249	1429	2129	0.253	1.30 (1.16-1.46)	5.64 × 10 ⁻⁶	
	Combined ^e											1.37 (1.23-1.50)	1.04 × 10 ⁻¹⁰	0.105
rs3135363														
	GWAS	c/t	No gene (6p21.3)	35	258	383	0.757	89	447	507	0.700	1.58 (1.32-1.90)	7.89 × 10 ⁻⁷	
	Replication			73	322	540	0.750	389	1486	1929	0.702	1.30 (1.16-1.46)	7.94 × 10 ⁻⁶	
	Combined ^e											1.37 (1.24-1.51)	1.45 × 10 ⁻¹⁰	0.069
rs3129860														
	GWAS	a/g	No gene (6p21.3)	58	294	324	0.303	57	348	638	0.221	1.55 (1.29-1.82)	6.45 × 10 ⁻⁶	
	Replication			88	339	507	0.276	208	1341	2246	0.231	1.28 (1.14-1.44)	2.53 × 10 ⁻⁵	
	Combined ^e											1.36 (1.22-1.49)	1.07 × 10 ⁻⁹	0.085

1618 (682 in GWAS and 936 in replication) liver cirrhosis and 4854 (1045 in GWAS and 3809 in replication) chronic hepatitis C samples were analyzed.

^aRAF, risk allele frequency.

^bOR, odds ratios; CI, confidence interval.

^cp Values obtained by logistic regression analysis adjusted for age and gender under additive model.

^dp Values of heterogeneities (Phet) across three stages were examined by using the Breslow-Day test.

^eCombined odds ratio and p values for independence test were calculated by Mendel-hauzen and Laird method in the meta-analysis.

Supplementary Fig. 3). To further evaluate the effect of each variation on the progression from CHC to LC, we performed multiple logistic regression analyses. As a result, rs910049 (p of 1.91×10^{-3} with OR of 1.25) and rs3135363 (p of 1.49×10^{-4} with OR of 1.23) remained significantly associated with the progression risk from CHC to LC, while the remaining three SNPs failed to show significant associations ($p > 0.05$) (Supplementary Table 3). Thus, two SNPs, rs910049 and rs3135363, seem to be independent risk factors for HCV-induced LC.

Since reduced platelet level is associated with a poor prognosis among CHC patients [44] we excluded patients with platelet level of less than 160,000 from CHC groups to increase the risk of type 2 error in this study. We also conducted the analysis using only CHC patients diagnosed with liver biopsy. As a result, both SNPs reached genome-wide significance ($p < 5 \times 10^{-8}$), although the associations were reduced due to the smaller sample size (Supplementary Table 4).

Subgroup analyses, stratified by IFN treatment status, amount of alcohol consumption, and gender, were also performed, since these factors were shown to be associated with the prognosis of CHC patients [45–47]. A total of 334 LC patients (35.83%) and 2325 CHC (82.4%) were treated with IFN therapy. Although the frequency of IFN treatment was different between CHC and LC groups, these variations associated with the LC risk regardless of IFN treatment as well as gender and alcohol consumption (Supplementary Fig. 4A–C). When we included these factors as covariates, the association of these variations with HCV-induced LC was sustained, with OR of 1.48 and 1.56, and SNP rs3135363

still reached genome-wide significance ($p = 3.95 \times 10^{-9}$) (Supplementary Table 5).

The association of previously reported variations with HCV-induced LC

Non-synonymous SNP rs738409 (I148M) in the *PNPLA3* gene was shown to be associated with progression of LC in the previous prospective study in Caucasians [31]. SNP rs738409 was also associated with the severity of non-alcoholic fatty liver disease in Japanese [48]. Therefore, we analyzed SNP rs738409 in our case-control cohort, but rs738409 did not significantly associate with HCV-induced LC ($p = 0.24$ and OR = 1.10), although the risk G allele was more frequent among LC than CHC (Supplementary Table 6). Our result is similar to what observed among Caucasians in the previous study, in which rs738409 increased liver cancer risk among alcoholic cirrhosis but did not among hepatitis C cirrhosis [49]. Since biological studies demonstrated that its risk allele (G) abolishes the triglyceride hydrolysis activity of *PNPLA3* [50] *PNPLA3* variation would have a strong impact on non-viral cirrhosis.

Recently, GWAS in the Caucasian population identified the association of SNPs rs4374383, rs16851720 and rs9380516 with the progression of liver fibrosis after HCV infection [51]. However, SNPs rs4374383 and rs16851720 did not exhibit significant association ($p = 0.654$ and 0.231 , respectively) in our sample set. Although SNP rs9380516 exhibited the association with p -value of 0.015, the risk allele showed an opposite result

Table 3. Results of three associated variations from candidate gene analyses.

Gene	Tagging SNP	Haplotype frequency		OR (95% CI) ^a	p value ^b	
		Liver cirrhosis	Chronic hepatitis C			
<i>DQA1*0601</i>	rs2736182(T) + rs2071293(A)	0.038	0.019	2.80	1.38-3.32	4.53 × 10 ⁻⁴
<i>DRB1*0405</i>	rs411326(C) + rs2395185(A) + rs4599680(A)	0.324	0.266	1.45	1.15-1.56	1.54 × 10 ⁻⁴

Association was tested by comparing haplotype distribution between 682 liver cirrhosis and 1045 chronic hepatitis C samples in GWAS.

^aOR, odds ratio; CI, confidence interval.

^bp Values were obtained by case-control analysis of GWAS stage (p for haplotype were obtained by score test, implemented in R) (*DQA1*0601* and *DRB1*0405*). The p values obtained by logistic regression analysis adjusted for age and gender under additive model.

(Supplementary Table 6). Taken together, these SNPs would not be associated with liver fibrosis in the Japanese population.

Genes related to extracellular matrix turnover or immune response (*KRT 19*, *COL1A1*, *STMN2*, *CXCL6*, *CCR2*, *TIMP1*, *IL8*, *IL1A*, *ITGA2*, *CLDN 4*, and *IL2*) were shown to be implicated in liver fibrosis of chronic hepatitis C [14]. To further characterize these loci, we conducted imputation analyses in the GWAS sample set (682 cases and 1045 controls), using data from HAPMAP phase II (JPT), and found 163 SNPs in 9 loci. However, none of these SNPs indicated significant association with p-value of less than 0.01 (Supplementary Table 7). Thus, variations of these genes did not associate with progression from chronic hepatitis C to liver cirrhosis.

Imputation-based fine mapping of HLA region

The most significantly associated SNP rs3135363 is located within an intergenic region between *BTNL2* and *HLA-DRA*, and rs910049 is located in intron 7 of *C6orf10* gene (Supplementary Figs. 5 and 6). To further characterize these loci, we conducted imputation-based association analysis for the GWAS samples (682 LC and 1045 CHC samples) using data from HAPMAP Phase II (JPT), and could obtain the results of nearly 6000 SNPs in a 4-Mb genomic region. The regional association plots revealed that all modestly-associated SNPs are confined within a 700-kb region containing 21 genes, namely *TNXB*, *ATF6B*, *FKBPL*, *PRRT1*, *PPT2*, *EGFL8*, *AGPAT1*, *RNF5*, *RNF5P1*, *AGER*, *PBX2*, *C6orf10*, *BTNL2*, *HLA-DRA*, *HLA-DRB5*, *HLA-DRB6*, *HLA-DRB1*, *HLA-DQA1*, *HLA-DQA2*, *HLA-DQB1* and *HLA-DQB2* (Supplementary Fig. 5). Although 640 SNPs, including ten non-synonymous SNPs within the 4-Mb region, showed very modest associations ($p < 0.01$) with HCV-induced LC, none of these SNPs in this region revealed strong association with HCV-induced LC, after adjustment with the two SNPs, rs910049 and rs3135363 (Supplementary Fig. 7). Taken together, the associations observed in this region would reflect the association with rs910049 and rs3135363.

Previous reports indicated the association of *HLA-DRB1* and *HLA-DQ* alleles with HCV-induced chronic hepatitis in the Japanese population [26]. To investigate the association of HLA alleles with HCV-induced LC, we estimated the genotypes at the HLA region by applying the imputation results of HLA-tagging SNPs [37]. We could successfully determine 53 alleles of *HLA-A*, *B*, *C*, *DQA*, *DQB*, and *DRB* genes and find that *HLA-DQA1*0601* and *HLA-DRB1*0405* were strongly associated with HCV-induced LC (p values of 4.53×10^{-4} and 1.54×10^{-4} with ORs of 2.80 and 1.45) even after the Bonferroni correction ($p < 0.05/53 = 9.43 \times 10^{-4}$) (Table 3 and Supplementary Table 8A-E) [37].

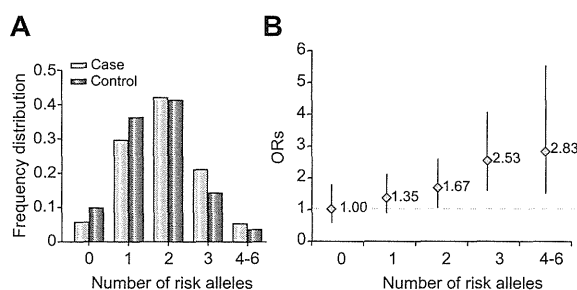


Fig. 2. Cumulative effects of liver cirrhosis risk alleles. (A) Frequency distribution divided by risk allele numbers (rs910049, rs3135353, and *HLA-DQA0601*) among liver cirrhosis (light blue bars) and chronic hepatitis C (dark blue bars) patients. (B) Plot of the increase odds ratio (OR) for liver cirrhosis according to the number of risk alleles. The ORs are relative to the subjects with no risk alleles (rs910049, rs3135353, and *HLA-DQA0601*). Vertical bars correspond to 95% confidence intervals. Horizontal line marks the null value (OR = 1).

Cumulative effect of multiple loci within the HLA region

SNPs rs3135363 and rs910049, *HLA-DQA1*0601*, and *HLA-DRB1*0405* are located within a 300-kb segment in the HLA class II region and show moderate linkage disequilibrium (Supplementary Fig. 8). To further evaluate these genetic factors, we performed multiple logistic regression analyses and found that rs910049 (p of 9.40×10^{-3} with OR of 1.38), rs3135363 (p of 3.94×10^{-4} with OR = 1.41), and *HLA-DQA1*0601* (p of 7.79×10^{-3} with OR of 1.54) were significantly associated with HCV-induced LC (Supplementary Table 9), indicating these three variations were independent risk factors for progression of CHC to LC.

To investigate the pathophysiological roles of rs910049 and rs3135363 in disease progression, we searched the eQTL database (<http://www.sph.umich.edu/csg/liang/imputation>) and found that risk alleles of rs910049 (A) and rs3135363 (T) were associated with lower expression of *HLA-DQA* (LOD of ≥ 6.86 and 17.31, respectively) and *DRB1* (LOD of ≥ 12.01 and 18.96, respectively), and with higher expression of *HLA-DQB1* (LOD of ≥ 6.76 and 4.46, respectively) (Supplementary Table 10). Thus, rs910049 and rs3135363 are likely to affect the expression of HLA class II molecules and subsequently alter the risk of HCV-induced LC.

Finally, we examined the cumulative effects of rs910049, rs3135363, and *HLA-DQA1*0601*. Individuals with four or more risk alleles (8.8% of general population) have 2.83-fold higher risk of HCV-induced LC compared with those with no risk allele (15.0% of general population, Fig. 2).

Research Article

Discussion

We here demonstrated that multiple genetic variations in the MHC region were significantly associated with the risk of disease progression from CHC to LC, using a total of 1618 HCV-LC and 4854 CHC cases. Since a substantial proportion of patients with CHC show progression to LC in a certain time period, exclusion of CHC patients who have a high risk for LC from control subjects is essential to reduce the risk of false negative association. In this study, CHC patients with advanced fibrosis (F3 or F4 in stage) or with reduced platelet level (less than 160,000/ μ l) were excluded from the control samples, since these alterations are well-known risk factors for LC development [9,32]. Consequently, we were successfully able to identify the HCV-induced LC loci.

HLA genes are known to play critical roles in the regulation of our immune responses through controlling the antigen presentation to CD8 (class I) and CD4 (class II) T cells. Although previous studies indicated the association of HLA class I alleles such as *HLA-B57*, *HLA-A11*, and *HLA-C04* with persistent HCV infection [52,53], no SNPs in the HLA class I region exhibited strong association with HCV-induced LC. Here we identified three variations (rs910049, rs3135363, *HLA-DQA1*0601*) in the HLA class II region to be significantly associated with the progression risk from CHC to LC. Since two SNPs, rs910049 and rs3135363, had been indicated to affect expression levels of *HLA-DRB1* and *DQ*, our findings indicated the significant pathophysiological roles of HLA class II molecules in the development of HCV-induced liver fibrosis. Considering the function of *HLA-DQ* and *HLA-DR*, we suggest that the antigen presentation by HLA class II molecules is likely to play a critical role in the elimination of HCV-infected liver cells and subsequently prevent HCV-induced LC.

Direct acting antiviral drugs for HCV can cure up to 75% of patients infected with HCV genotype 1, and the lifetime risk of developing LC and HCC among HCV carriers was decreased during the two recent decades [54,13]. However, the amino acid sequence of the NS3 protease domain varies significantly between HCV genotypes and the antiviral efficacy differs in different HCV genotypes [55]. Moreover, protease inhibitors increased the incidence of adverse reactions such as anemia and skin rash [56]. Therefore, estimation of liver cirrhosis risk and prediction of treatment response would be essential to provide a personalized treatment and to achieve the optimal results. Due to the recent advances in pharmacogenetic studies, genetic factors associated with efficacy and adverse effects of anti-HCV treatment were identified. *IL-28B* is a powerful predictor of treatment outcome of pegylated interferon and ribavirin therapy [22], while a genetic variation in the *ITPA* gene was shown to be associated with ribavirin-induced anemia [57]. Since we conducted a retrospective study, and the majority of LC patients did not receive IFN treatment, we could not evaluate the treatment responses in our study design. However, SNPs identified in this study were associated with the LC risk independent of IFN treatment. Although the impact of each SNP was relatively weak compared with viral factors (HCV genotype, core and NS5A mutation [58]) and host factors (age, gender, obesity, and insulin resistance), we found that individuals with three or more risk alleles have a nearly three-fold higher risk of LC than those with no risk allele. Since lifetime risk of HCC development among HCV carriers is as high as about 27% for male and 8% for female [59], these three loci would have the strong effect on the clinical outcome of CHC patients. In general, the progression from chronic hepatitis C to liver cirrhosis usually takes more than 20–30 years. Therefore,

a large scale prospective cohort study with more than 10-year follow-up is essential to evaluate the role of these variations as a prognostic biomarker. We would like to perform prospective analysis in future studies. We hope that our findings would contribute to clarify the underlying molecular mechanism of HCV-induced liver cirrhosis.

Financial support

This work was conducted as a part of the BioBank Japan Project that was supported by the Ministry of Education, Culture, Sports, Science and Technology of the Japanese government.

Conflict of interest

The authors who have taken part in this study declared that they do not have anything to disclose regarding funding or conflict of interest with respect to this manuscript.

Authors' contributions

Y. U., K. K., K. C., and K.M. conceived and designed the study; Y. U., H. O., N. K., Y. K., R. M., N. H., and M. K. performed genotyping; A. T., P. H. Y. L., C. T., and N. K. performed quality control at genome-wide phase; M. O., R. T., M. O., K. K., D. M., H. A., J. T., H. K., Y. N., K. M. and M. K. managed DNA samples; Y. U. analyzed and summarized the whole results; Y. U., Y. N., and K. M. wrote the manuscript; Y. N. obtained funding for the study.

Acknowledgments

We thank Ayako Matsui and Hiroe Tagaya (the University of Tokyo), and the technical staff of the Laboratory for Genotyping Development, Center for Genomic Medicine, RIKEN, for their technical support.

Supplementary data

Supplementary data associated with this article can be found, in the online version, at <http://dx.doi.org/10.1016/j.jhep.2012.12.024>.

References

- [1] Shepard CW, Finelli L, Alter MJ. Global epidemiology of hepatitis C virus infection. *Lancet Infect Dis* 2005;5:558–567.
- [2] Seeff LB. Natural history of chronic hepatitis C. *Hepatology* 2002;36:S35–S46.
- [3] Thomas DL, Seeff LB. Natural history of hepatitis C. *Clin Liver Dis* 2005;9:383–398, vi.
- [4] Freeman AJ, Dore GJ, Law MG, Thorpe M, Von Overbeck J, Lloyd AR, et al. Estimating progression to cirrhosis in chronic hepatitis C virus infection. *Hepatology* 2001;34:809–816.
- [5] Hoofnagle JH. Hepatitis C: the clinical spectrum of disease. *Hepatology* 1997;26:155–205.
- [6] Tanaka H, Imai Y, Hiramatsu N, Ito Y, Imanaka K, Oshita M, et al. Declining incidence of hepatocellular carcinoma in Osaka, Japan, from 1990 to 2003. *Ann Intern Med* 2008;148:820–826.

JOURNAL OF HEPATOLOGY

- [7] Global burden of disease (GBD) for hepatitis C. *J Clin Pharmacol* 2004;44:20–29.
- [8] Poyndar T, Bedossa P, Opolon P. Natural history of liver fibrosis progression in patients with chronic hepatitis C. The OBSVIRC, METAVIR, CLINIVIR, and DOSVIRC groups. *Lancet* 1997;349:825–832.
- [9] Yoshida H, Shiratori Y, Moriyama M, Arakawa Y, Ide T, Sata M, et al. Interferon therapy reduces the risk for hepatocellular carcinoma: national surveillance program of cirrhotic and noncirrhotic patients with chronic hepatitis C in Japan. IJIT Study Group. Inhibition of hepatocarcinogenesis by interferon therapy. *Ann Intern Med* 1999;131:174–181.
- [10] Zhang Q, Tanaka K, Sun P, Nakata M, Yamamoto R, Sakimura K, et al. Suppression of synaptic plasticity by cerebrospinal fluid from anti-NMDA receptor encephalitis patients. *Neurobiol Dis* 2012;45:610–615.
- [11] Aghemo A, Prati GM, Rumi MG, Soffredini R, D'Ambrosio R, Orsi E, et al. A sustained virological response prevents development of insulin resistance in chronic hepatitis C patients. *Hepatology* 2012;56:549–556.
- [12] Bièche I, Asselah T, Laurendeau I, Vidaud D, Degot C, Paradis V, et al. Molecular profiling of early stage liver fibrosis in patients with chronic hepatitis C virus infection. *Virology* 2005;332:130–144.
- [13] Estrabaud E, Vidaud M, Marcellin P, Asselah T. Genomics and HCV infection: progression of fibrosis and treatment response. *J Hepatol* 2012;57:1110–1125.
- [14] Asselah T, Bièche I, Laurendeau I, Paradis V, Vidaud D, Degot C, et al. Liver gene expression signature of mild fibrosis in patients with chronic hepatitis C. *Gastroenterology* 2005;129:2064–2075.
- [15] Marquez RT, Bandyopadhyay S, Wendlandt EB, Keck K, Hoffer BA, Icardi MS, et al. Correlation between microRNA expression levels and clinical parameters associated with chronic hepatitis C viral infection in humans. *Lab Invest* 2010;90:1727–1736.
- [16] Morita K, Taketomi A, Shirabe K, Umeda K, Kayashima H, Ninomiya M, et al. Clinical significance and potential of hepatic microRNA-122 expression in hepatitis C. *Liver Int* 2011;31:474–484.
- [17] Cui R, Okada Y, Jang SG, Ku JL, Park JG, Kamatani Y, et al. Common variant in 6q26-q27 is associated with distal colon cancer in an Asian population. *Gut* 2011;60:799–805.
- [18] Kumar V, Matsuo K, Takahashi A, Hosono N, Tsunoda T, Kamatani N, et al. Common variants on 14q32 and 13q12 are associated with DLBCL susceptibility. *J Hum Genet* 2011;56:436–439.
- [19] Tanikawa C, Urabe Y, Matsuo K, Kubo M, Takahashi A, Ito H, et al. A genome-wide association study identifies two susceptibility loci for duodenal ulcer in the Japanese population. *Nat Genet* 2012;44:430–434.
- [20] Urabe Y, Tanikawa C, Takahashi A, Okada Y, Morizono T, Tsunoda T, et al. A genome-wide association study of nephrolithiasis in the Japanese population identifies novel susceptible loci at 5q35.3, 7p14.3, and 13q14.1. *PLoS Genet* 2012;8:e1002541.
- [21] Thomas DL, Thio CL, Martin MP, Qi Y, Ge D, O'Huigin C, et al. Genetic variation in IL28B and spontaneous clearance of hepatitis C virus. *Nature* 2009;461:798–801.
- [22] Tanaka Y, Nishida N, Sugiyama M, Kurosaki M, Matsuura K, Sakamoto N, et al. Genome-wide association of IL28B with response to pegylated interferon-alpha and ribavirin therapy for chronic hepatitis C. *Nat Genet* 2009;41:1105–1109.
- [23] Suppiah V, Moldovan M, Ahlenstiel G, Berg T, Weltman M, Abate ML, et al. IL28B is associated with response to chronic hepatitis C interferon-alpha and ribavirin therapy. *Nat Genet* 2009;41:1100–1104.
- [24] Kumar V, Kato N, Urabe Y, Takahashi A, Muroyama R, Hosono N, et al. Genome-wide association study identifies a susceptibility locus for HCV-induced hepatocellular carcinoma. *Nat Genet* 2011;43:455–458.
- [25] Miki D, Ochi H, Hayes CN, Abe H, Yoshima T, Aikata H, et al. Variation in the DEPDC5 locus is associated with progression to hepatocellular carcinoma in chronic hepatitis C virus carriers. *Nat Genet* 2011;43:797–800.
- [26] Kuzushita N, Hayashi N, Moribe T, Katayama K, Kanto T, Nakatani S, et al. Influence of HLA haplotypes on the clinical courses of individuals infected with hepatitis C virus. *Hepatology* 1998;27:240–244.
- [27] Singh R, Kaul R, Kaul A, Khan K. A comparative review of HLA associations with hepatitis B and C viral infections across global populations. *World J Gastroenterol* 2007;13:1770–1787.
- [28] Mosaad YM, Farag RE, Arafat MM, Eletreby S, El-Alfy HA, Eldeek BS, et al. Association of human leucocyte antigen Class I (HLA-A and HLA-B) with chronic hepatitis C virus infection in Egyptian patients. *Scand J Immunol* 2010;72:548–553.
- [29] Li CZ, Kato N, Chang JH, Muroyama R, Shao RX, Dharel N, et al. Polymorphism of OAS-1 determines liver fibrosis progression in hepatitis C by reduced ability to inhibit viral replication. *Liver Int* 2009;29:1413–1421.
- [30] Mozer-Lisewska I, Sikora J, Kowala-Piaskowska A, Kaczmarek M, Dworacki G, Zeromski J. The incidence and significance of pattern-recognition receptors in chronic viral hepatitis types B and C in man. *Arch Immunol Ther Exp (Warsz)* 2010;58:295–302.
- [31] Trépo E, Pradat P, Pothoff A, Momozawa Y, Quertinmont E, Gustot T, et al. Impact of patatin-like phospholipase-3 (rs738409 C>G) polymorphism on fibrosis progression and steatosis in chronic hepatitis C. *Hepatology* 2011;54:60–69.
- [32] Romero-Gómez M, Gómez-González E, Madrazo A, Vera-Valencia M, Rodrigo L, Pérez-Alvarez R, et al. Optical analysis of computed tomography images of the liver predicts fibrosis stage and distribution in chronic hepatitis C. *Hepatology* 2008;47:810–816.
- [33] Nakamura Y. The BioBank Japan project. *Clin Adv Hematol Oncol* 2007;5:696–697.
- [34] Purcell S, Neale B, Todd-Brown K, Thomas L, Ferreira M, Bender D, et al. PLINK: a tool set for whole-genome association and population-based linkage analyses. *Am J Hum Genet* 2007;81:559–575.
- [35] Frazer KA, Ballinger DG, Cox DR, Hinds DA, Stuve LL, Gibbs RA, et al. A second generation human haplotype map of over 3.1 million SNPs. *Nature* 2007;449:851–861.
- [36] Breslow NE, Day NE. Statistical methods in cancer research. The design and analysis of cohort studies. *IARC Sci Publ* 1987;11:1–406.
- [37] de Bakker PI, McVean G, Sabeti PC, Miretti MM, Green T, Marchini J, et al. A high-resolution HLA and SNP haplotype map for disease association studies in the extended human MHC. *Nat Genet* 2006;38:1166–1172.
- [38] Scott LJ, Mohlke KL, Bonnycastle LL, Willer CJ, Li Y, Duren WL, et al. A genome-wide association study of type 2 diabetes in Finns detects multiple susceptibility variants. *Science* 2007;316:1341–1345.
- [39] Consortium GP. A map of human genome variation from population-scale sequencing. *Nature* 2010;467:1061–1073.
- [40] Barrett J, Fry B, Maller J, Daly M. Haploview: analysis and visualization of LD and haplotype maps. *Bioinformatics* 2005;21:263–265.
- [41] Xu Z, Taylor JA. SNPinfo: integrating GWAS and candidate gene information into functional SNP selection for genetic association studies. *Nucleic Acids Res* 2009;37:W600–W605.
- [42] Dixon AL, Liang L, Moffatt MF, Chen W, Heath S, Wong KC, et al. A genome-wide association study of global gene expression. *Nat Genet* 2007;39:1202–1207.
- [43] Kel AE, Gössling E, Reuter I, Chermushkin E, Kel-Margoulis OV, Wingender E. MATCH: a tool for searching transcription factor binding sites in DNA sequences. *Nucleic Acids Res* 2003;31:3576–3579.
- [44] Wai CT, Greenon JK, Fontana RJ, Kalbfleisch JD, Marrero JA, Conjeevaram HS, et al. A simple noninvasive index can predict both significant fibrosis and cirrhosis in patients with chronic hepatitis C. *Hepatology* 2003;38:518–526.
- [45] Cammà C, Di Bona D, Schepis F, Heathcote EJ, Zeuzem S, Pockros PJ, et al. Effect of peginterferon alfa-2a on liver histology in chronic hepatitis C: a meta-analysis of individual patient data. *Hepatology* 2004;39:333–342.
- [46] Marcellin P, Asselah T, Boyer N. Fibrosis and disease progression in hepatitis C. *Hepatology* 2002;36:S47–S56.
- [47] Silini E, Bottelli R, Asti M, Bruno S, Candusso ME, Brambilla S, et al. Hepatitis C virus genotypes and risk of hepatocellular carcinoma in cirrhosis: a case-control study. *Gastroenterology* 1996;111:199–205.
- [48] Kawaguchi T, Sumida Y, Umamura A, Matsuo K, Takahashi M, Takamura T, et al. Genetic polymorphisms of the human PNPLA3 gene are strongly associated with severity of non-alcoholic fatty liver disease in Japanese. *PLoS One* 2012;7:e38322.
- [49] Nischalke HD, Berger C, Luda C, Berg T, Müller T, Grünhage F, et al. The PNPLA3 rs738409 148M/I genotype is a risk factor for liver cancer in alcoholic cirrhosis but shows no or weak association in hepatitis C cirrhosis. *PLoS One* 2011;6:e27087.
- [50] He S, McPhaul C, Li JZ, Garuti R, Kinch L, Grishin NV, et al. A sequence variation (1148M) in PNPLA3 associated with nonalcoholic fatty liver disease disrupts triglyceride hydrolysis. *J Biol Chem* 2010;285:6706.
- [51] Patin E, Kutalik Z, Guernon J, Bibert S, Nalpas B, Jouanguy E, et al. Genome-wide association study identifies variants associated with progression of liver fibrosis from HCV infection. *Gastroenterology* 2012;143:124–152, e1–12.
- [52] Kim AY, Kuntzen T, Timm J, Nolan BE, Baca MA, Reyrol LL, et al. Spontaneous control of HCV is associated with expression of HLA-B 57 and preservation of targeted epitopes. *Gastroenterology* 2011;140:e681.
- [53] Fanning LJ, Kenny-Walsh E, Shanahan F. Persistence of hepatitis C virus in a white population: associations with human leukocyte antigen class 1. *Hum Immunol* 2004;65:745–751.

Research Article

- [54] Imhof I, Simmonds P. Genotype differences in susceptibility and resistance development of hepatitis C virus to protease inhibitors telaprevir (VX-950) and danoprevir (ITMN-191). *Hepatology* 2011;53:1090–1099.
- [55] Asselah T, Marcellin P. Direct acting antivirals for the treatment of chronic hepatitis C: one pill a day for tomorrow. *Liver Int* 2012;32:88–102.
- [56] Ozeki I, Akaike J, Karino Y, Arakawa T, Kuwata Y, Ohmura T, et al. Antiviral effects of peginterferon alpha-2b and ribavirin following 24-week monotherapy of telaprevir in Japanese hepatitis C patients. *J Gastroenterol* 2011;46:929–937.
- [57] Ochi H, Maekawa T, Abe H, Hayashida Y, Nakano R, Kubo M, et al. ITPA polymorphism affects ribavirin-induced anemia and outcomes of therapy – a genome-wide study of Japanese HCV virus patients. *Gastroenterology* 2010;139:1190–1197.
- [58] Enomoto N, Sakuma I, Asahina Y, Kurosaki M, Murakami T, Yamamoto C, et al. Mutations in the nonstructural protein 5A gene and response to interferon in patients with chronic hepatitis C virus 1b infection. *N Engl J Med* 1996;334:77–82.
- [59] Huang YT, Jen CL, Yang HI, Lee MH, Su J, Lu SN, et al. Lifetime risk and sex difference of hepatocellular carcinoma among patients with chronic hepatitis B and C. *J Clin Oncol* 2011;29:3643–3650.

Knockdown of Receptor-Interacting Serine/Threonine Protein Kinase-2 (RIPK2) Affects EMT-associated Gene Expression in Human Hepatoma Cells

SHUANG WU, TATSUO KANDA, SHINGO NAKAMOTO, FUMIO IMAZEKI and OSAMU YOKOSUKA

*Department of Medicine and Clinical Oncology, Chiba University,
Graduate School of Medicine, Chuo-ku, Chiba, Japan*

Abstract. *Background: Receptor-interacting serine/ threonine protein kinase-2 (RIPK2) has been reported to be an important regulator of tumor proliferation, differentiation and wound repair. We investigated the effects of RIPK2 knockdown in human hepatoma cells on epithelial-to-mesenchymal transition (EMT)-associated gene expression. Materials and Methods: HepG2 cells stably expressing RIPK2-shRNA (HepG2-shRIPK2) were generated after puromycin selection. Total RNAs from HepG2-shRIPK2 and from HepG2-shcontrol cells were isolated and PCR-based arrays were performed to compare the 84 EMT-associated gene expressions. Results: We observed that knockdown of RIPK2 down-regulated mRNA expression of jagged 1 (JAG1); plasminogen activator inhibitor-1 (PAI1); regulator of G-protein signalling 2, 24 kDa (RGS2); E-cadherin (CDH1); fibroblast growth factor binding protein 1 (FGFBP1); snail homolog 2 (SNAIL2); protein tyrosine phosphatase type IVA, member 1 (PTP4A1); keratin 19 (KRT19); vimentin (VIM); and survival of motor neuron protein-interacting protein 1 (SIP1). Conclusion: We found that knockdown of RIPK2 down-regulated nuclear factor kappa B (NF- κ B)-dependent PAI1 and VIM gene expressions. RIPK2 might play an important role in hepatic cell migration. These findings could shed new light on carcinogenesis and on liver regeneration.*

Receptor-interacting protein (RIP) family kinases have emerged as essential sensors of cellular stress (1). RIP kinases (RIPKs) are closely related to members of the interleukin-1-receptor-associated kinase (IRAK) family. To date, five RIPKs are known (2). They play important roles in situations of

cellular stress caused by different factors, such as pathogen infection, inflammation, cellular differentiation programs and DNA damage, and eventually lead to the activation of transcription factors, such as nuclear factor kappa B (NF- κ B), the induction of apoptotic processes, or activation of mitogen-activated protein kinase (MAPK) (1, 2).

Our group as well as others showed that receptor-interacting serine/ threonine protein kinase-2 (RIPK2, also known as RIP2, RICK or CARDIAK), a caspase-recruitment domain-containing kinase, plays an important role in cell migration and wound healing in keratinocytes as well as hepatocytes (2, 3). RIPK2 is also involved in the Toll-like receptor (TLR)-signalling pathway and plays an important role in the production of inflammatory cytokines through NF- κ B activation (4, 5). RIPK2 also plays an important role in nucleotide-binding oligomerization domain containing 1 (NOD1) ligand-induced NF- κ B activation in hepatocytes (3).

The extracellular matrix (ECM), which consists of collagens, glycoproteins, proteoglycans and glycosaminoglycans, provides cells with positional information and a mechanical scaffold for adhesion and migration. Chronic fibrogenesis can be regarded as a continuous wound-healing process that results in scar formation (6). Dynamic interactions between growth factors and the ECM are integral to wound healing (7, 8). Wound healing, and inflammatory processes, as well as changes in the tumor microenvironment through remodeling of the ECM, are important for cancer metastasis (8). The epithelial-to-mesenchymal transition (EMT) now takes center stage as the convergence point between inflammation and the progression of degenerative fibrotic diseases and cancer (9). EMT includes many processes associated with differentiation and development, morphogenesis, cell growth and proliferation, migration and motility, cytoskeleton formation, ECM and cell adhesion, and related signalling pathways, as well as transcription factors. The NF- κ B family of transcription factors plays pivotal roles in both promoting and maintaining the cell phenotype (9, 10). Inflammation is necessary for EMT (11), and NF- κ B plays an important role in the induction of inflammation (12).

Correspondence to: Associate Professor Tatsuo Kanda, MD, Ph.D., Department of Medicine and Clinical Oncology, Chiba University, Graduate School of Medicine, 1-8-1 Inohana, Chuo-ku, Chiba 260-8670, Japan. Tel: +81 432262086, Fax: +81 432262088, e-mail: kandat-cib@umin.ac.jp

Key Words: EMT, HCC, NF- κ B, RIPK2, hepatoma cells.

In the present study, we uncovered a novel function of endogenous RIPK2, which is located upstream of NF- κ B. Knockdown of *RIPK2* in human hepatoma cells affected EMT-associated gene expression.

Materials and Methods

Cell culture. Human hepatoblastoma HepG2 cells were maintained in Dulbecco's modified Eagle's medium (Sigma-Aldrich, St. Louis, MO, USA) with 10% fetal bovine serum under 5% CO₂, at 37°C.

Transfection of cells. HepG2 cells were transfected with plasmid control-shRNA or *RIPK2*-shRNA (Santa Cruz Biotechnology, CA, USA). After 48 h of transfection, cells were split and treated with puromycin for selection of antibiotic-resistant colonies. Individual colonies were picked-up and examined for expression of endogenous *RIPK2* by western blotting with specific antibodies against *RIPK2* (3), and clones HepG2-shC and HepG2-shRIPK2 [HepG2-shRIPK2-3 (3)], in which *RIPK2* expression was knocked-down, were selected for subsequent studies.

RNA extraction. Cells were seeded into 6-well plates, and total cellular RNA was extracted 48 h later, using the RNeasy Mini kit (Qiagen, Tokyo, Japan) according to the manufacturer's instructions. RNA samples were then stored at -80°C until use. RNA quality was examined using the A₂₈₀/A₂₆₀ ratio (Pharmacia Biotech, Bedford, MA, USA).

cDNA synthesis and real-time polymerase chain reaction (PCR). cDNA synthesis was performed using RT² First Strand Kit (SABiosciences, Frederick, MD, USA). Each 1 μ g of RNA was subjected to one reaction. The cDNA synthesis reaction was performed as follows: incubation at 42°C for 15 min and then reaction stoppage by heating at 95°C for 15 min. RNA quantification was conducted by real-time PCR with SyBr Green I, as described previously (12, 13). Gene quantification was determined using an ABI Prism 7300 instrument from Applied Biosystems (Foster City, CA, USA). Thermal cycling conditions were 95°C for 10 min, followed by 40 cycles at 95°C, 15 s for denaturation, and 1 min at 60°C for annealing and extension. All primers for examining human EMT-associated gene expression were purchased from SABiosciences. EMT-associated genes examined in the present study are listed in Table I. Gene expression was normalized to that of house-keeping genes (beta-2-microglobulin, hypoxanthine phosphoribosyltransferase 1, ribosomal protein L 13a, glyceraldehyde-3-phosphate dehydrogenase and beta-actin) to determine the fold-change in gene expression between test (HepG2-shRIPK2) and control (HepG2-shC) samples by the 2^{- $\Delta\Delta$ CT} (comparative cycle threshold) method (13). We performed each of these experiments in triplicate. Genes were annotated by Entrez Gene (NCBI, Bethesda, MD, USA).

Statistical analysis. Data were analyzed with RT² profiler PCR array data analysis software (<http://www.superarray.com/pcrarraydataanalysis.php>).

Results

Down-regulated genes among EMT-associated genes in *RIPK2*-knockdown HepG2 cells. *RIPK2* functions as a signal transducer for both the innate and adaptive immune activation pathways (14). In our previous study, we observed that *RIPK2*

plays an important role in cell migration and wound healing in hepatocytes (3). We examined EMT-associated gene expression profiles using real-time PCR-based focused microarrays. A comparison of EMT-associated genes between HepG2-shC and HepG2-shRIPK2 is shown in Tables II and III. Among the 84 EMT-associated genes examined, collagen, type 1, alpha 2 gene (*COL1A2*) was undetected in both types of samples and the average threshold cycle of 12 genes was relatively high (>30), meaning that their relative expression level was low. We thus excluded these 13 genes from further analysis. Out of the remaining 71 genes, 10 (14.0%) were significantly down-regulated by the knockdown of *RIPK2* ($p < 0.05$; Table II). Among these 10 genes, six [jagged 1 (*JAG1*); plasminogen activator inhibitor-1 (*PAI1*); regulator of G-protein signalling 2, 24 kDa (*RGS2*); E-cadherin (*CDH1*); fibroblast growth factor binding protein 1 (*FGFBP1*); and snail homolog 2 (*SNAI2*)] were down-regulated by 1.5-fold or more in HepG2-shRIPK2 cells.

Up-regulated genes among EMT-associated genes in *RIPK2*-knockdown HepG2 cells. Out of the remaining 71 genes, six (8.4%) were significantly up-regulated by the knock-down of *RIPK2* ($p < 0.05$; Table III). Out of these six genes, four [collagen, type V, alpha 2 (*COL5A2*); matrix metalloproteinase 2 (MMP2); MMP3; and goosecoid homeobox (*GSC*)] were up-regulated by 1.5-fold or more in HepG2-shRIPK2 cells.

Discussion

In the present study, we observed that 10 genes were significantly down-regulated in HepG2-shRIPK2 cells. Out of these 10 genes, *PAI1* and vimentin (*VIM*) are NF- κ B-dependent genes (15, 16). We also observed 6 genes were significantly up-regulated in HepG2-shRIPK2 cells. It was reported that NF- κ B is involved in the expression of the wingless-type mouse mammary tumor virus (MMTV) integration site family, member 5B (*WNT5B*), MMP2 and MMP3 (17-19). Our previous study (3) showed that knockdown of *RIPK2* has an effect on NOD1 ligand C12-iE-DAP-induced NF- κ B activation in HepG2 cells, suggesting that *RIPK2* plays an important role in NF- κ B activation induced through NOD1 triggering in hepatocytes. We also observed that silencing of *RIPK2* was associated with the reduction of interleukin-6 (IL6), IL8 and hepatic wound closure (3).

PAI1, a multifaceted proteolytic factor, plays an important role in the plasminogen/plasmin system as it is the main inhibitor of tissue-type and urokinase-type plasminogen activator (20). *PAI1* also plays an important role in signal transduction, cell adherence and cell migration (21). It was reported that *PAI1* is associated with poor prognosis in several types of cancers (21) and that it is associated with hepatocellular carcinoma (HCC) caused by hepatitis B and C (22). Recently, single-nucleotide polymorphism (SNP) of

Table 1. *Genes associated with epithelial-to-mesenchymal transition (EMT) assessed by real-time RT-PCR in the present study.*

Genes up-regulated during EMT

Symbol	Name
<i>AHNAK</i>	AHNAK nucleoprotein
<i>BMP1</i>	Bone morphogenetic protein 1
<i>CALD1</i>	Caldesmon 1
<i>CAMK2N1</i>	Calcium/calmodulin-dependent protein kinase II inhibitor
<i>CDH2</i>	Cadherin 2, type 1, N-cadherin (neuronal)
<i>COL1A2</i>	Collagen, type I, alpha 2
<i>COL3A1</i>	Collagen type III, alpha 1
<i>COL5A2</i>	Collagen, type V, alpha 2
<i>FN1</i>	Fibronectin 1
<i>FOXC2</i>	Forkhead box C2 (MFH-1, mesenchyme forkhead 1)
<i>GNG11</i>	Guanine nucleotide binding protein (G protein), gamma 11
<i>GSC</i>	Goosecoid homeobox
<i>IGFBP4</i>	Insulin-like growth factor binding protein 4
<i>ITGA5</i>	Integrin, alpha 5 (fibronectin receptor, alpha polypeptide)
<i>ITGAV</i>	Integrin, alpha V (vitronectin receptor, beta polypeptide, antigen CD29 includes MDF2, MSK12)
<i>MMP2</i>	Matrix metalloproteinase 2 (gelatinase A, 72 kDa gelatinase, 72 kDa type IV collagenase)
<i>MMP3</i>	Matrix metalloproteinase 3 (stromelysin 1, progelatinase)
<i>MMP9</i>	Matrix metalloproteinase 9 (gelatinase B, 92 kDa gelatinase, 92 kDa type IV collagenase)
<i>MSN</i>	Moesin
<i>PAI1</i>	Plasminogen activator inhibitor type 1
<i>SNAI1</i>	Snail homolog 1 (<i>Drosophila</i>)
<i>SNAI2</i>	Snail homolog 2 (<i>Drosophila</i>)
<i>SNAI3</i>	Snail homolog 3 (<i>Drosophila</i>)
<i>SOX10</i>	SRY (sex-determining region Y)-box 10
<i>SPARC</i>	Secreted protein, acidic, cysteine-rich (osteonectin)
<i>STEAP1</i>	Six transmembrane epithelial antigen of the prostate 1
<i>TCF4</i>	Transcription factor 4
<i>TIMP1</i>	Tissue inhibitor of metalloproteinases-1
<i>TMEFF1</i>	Transmembrane protein with EGF-like and two follistatin-like domains 1
<i>TMEM132A</i>	Transmembrane protein 132A
<i>TWIST1</i>	Twist homolog 1 (<i>Drosophila</i>)
<i>VCAN</i>	Versican
<i>VIM</i>	Vimentin
<i>VPS13A</i>	Vacuolar protein sorting 13 homolog A (<i>Saccharomyces cerevisiae</i>)
<i>WNT5A</i>	Wingless-type MMTV integration site family, member 5A
<i>WNT5B</i>	Wingless-type MMTV integration site family, member 5B

Genes down-regulated during EMT

Symbol	Name
<i>CAV2</i>	Caveolin 2
<i>CDH1</i>	Cadherin 1, type 1, E-cadherin (epithelial)
<i>DSP</i>	Desmoplakin
<i>FGFBP1</i>	Fibroblast growth factor binding protein 1
<i>IL1RN</i>	Interleukin 1 receptor antagonist
<i>KRT19</i>	Keratin 19
<i>MITF</i>	Microphthalmia-associated transcription factor
<i>MST1R</i>	Macrophage stimulating 1 receptor (c-MET-related tyrosine kinase)
<i>NUDT13</i>	Nudix (nucleoside diphosphate linked moiety X)-type motif 13
<i>OCN</i>	Occludin
<i>PPPDE2</i>	PPPDE peptidase domain containing 2
<i>RGS2</i>	Regulator of G-protein signalling 2, 24 kDa
<i>SPP1</i>	Secreted phosphoprotein 1
<i>TFPI2</i>	Tissue factor pathway inhibitor 2
<i>TSPAN13</i>	Tetraspanin 13

continued

Table I. *continued.*

Differentiation and development

Symbol	Name
<i>AKT1</i>	V-akt murine thymoma viral oncogene homolog 1
<i>BMP1</i>	Bone morphogenetic protein 1
<i>BMP7</i>	Bone morphogenetic protein 7
<i>COL3A1</i>	Collagen, type III, alpha 1
<i>COL5A2</i>	Collagen, type V, alpha 2
<i>CTNNB1</i>	Catenin (cadherin-associated protein), beta 1, 88 kDa
<i>DSP</i>	Desmoplakin
<i>ERBB3</i>	V-erb-b2 erythroblastic leukemia viral oncogene homolog 3 (avian)
<i>F11R</i>	F11 receptor
<i>FOXC2</i>	Forkhead box C2 (MFH-1, mesenchyme forkhead 1)
<i>FZD7</i>	Frizzled homolog 7 (<i>Drosophila</i>)
<i>GSC</i>	Goosecoid homeobox
<i>JAG1</i>	Jagged 1 (Alagille syndrome)
<i>KRT14</i>	Keratin 14
<i>MITF</i>	Microphthalmia-associated transcription factor
<i>MST1R</i>	Macrophage-stimulating 1 receptor (c-MET-related tyrosine kinase)
<i>NODAL</i>	Nodal homolog (mouse)
<i>NOTCH1</i>	Notch homolog 1, translocation-associated (<i>Drosophila</i>)
<i>PTP4A1</i>	Protein tyrosine phosphatase type IVA, member 1
<i>SMAD2</i>	SMAD family member 2
<i>SNAI1</i>	Snail homolog 1 (<i>Drosophila</i>)
<i>SNAI2</i>	Snail homolog 2 (<i>Drosophila</i>)
<i>SOX10</i>	SRY (sex determining region Y)-box 10
<i>TGFB2</i>	Transforming growth factor, beta 2
<i>TGFB3</i>	Transforming growth factor, beta 3
<i>TMEFF1</i>	Transmembrane protein with EGF-like and two follistatin-like domains 1
<i>TWIST1</i>	Twist homolog 1 (<i>Drosophila</i>)
<i>VCAN</i>	Versican
<i>WNT11</i>	Wingless-type MMTV integration site family, member 11
<i>WNT5A</i>	Wingless-type MMTV integration site family, member 5A
<i>WNT5B</i>	Wingless-type MMTV integration site family, member 5B

Morphogenesis

Symbol	Name
<i>CTNNB1</i>	Catenin (cadherin-associated protein), beta 1, 88kDa
<i>FOXC2</i>	Forkhead box C2 (MFH-1, mesenchyme forkhead 1)
<i>JAG1</i>	Jagged 1 (Alagille syndrome)
<i>RAC1</i>	RAS-related C3 botulinum toxin substrate 1 (Rho family, small GTP binding protein RAC1)
<i>SMAD2</i>	SMAD family member 2
<i>SNAI1</i>	Snail homolog 1 (<i>Drosophila</i>)
<i>SOX10</i>	SRY (sex-determining region Y)-box 10
<i>TGFB1</i>	Transforming growth factor, beta 1
<i>TGFB2</i>	Transforming growth factor, beta 2
<i>TGFB3</i>	Transforming growth factor, beta 3
<i>TWIST1</i>	Twist homolog 1 (<i>Drosophila</i>)
<i>WNT11</i>	Wingless-type MMTV integration site family, member 11
<i>WNT5A</i>	Wingless-type MMTV integration site family, member 5A

Cell growth and proliferation

Symbol	Name
<i>AKT1</i>	V-akt murine thymoma viral oncogene homolog 1
<i>BMP1</i>	Bone morphogenetic protein 1

continued

Table I. *continued.*

Symbol	Name
<i>BMP7</i>	Bone morphogenetic protein 7
<i>CAV2</i>	Caveolin 2
<i>CTNNB1</i>	Catenin (cadherin-associated protein), beta 1, 88 kDa
<i>EGFR</i>	Epidermal growth factor receptor (erythroblastic leukemia viral (v-erb-b) oncogene homolog, avian)
<i>ERBB3</i>	V-erb-b2 erythroblastic leukemia viral oncogene homolog 3 (avian)
<i>FGFBP1</i>	Fibroblast growth factor binding protein 1
<i>FOXC2</i>	Forkhead box C2 (MEF-1, mesenchyme forkhead 1)
<i>IGFBP4</i>	Insulin-like growth factor binding protein 4
<i>ILK</i>	Integrin-linked kinase
<i>JAG1</i>	Jagged 1 (Alagille syndrome)
<i>MST1R</i>	Macrophage stimulating 1 receptor (c-MET-related tyrosine kinase)
<i>NODAL</i>	Nodal homolog (mouse)
<i>PDGFRB</i>	Platelet-derived growth factor receptor, beta polypeptide
<i>TGFB1</i>	Transforming growth factor, beta 1
<i>TGFB2</i>	Transforming growth factor, beta 2
<i>TGFB3</i>	Transforming growth factor, beta 3
<i>TIMP1</i>	Tissue inhibitor of metalloproteinases-1
<i>VCAN</i>	Versican
<i>ZEB1</i>	Zinc finger E-box binding homeobox 1
Migration and motility	
Symbol	Name
<i>CALD1</i>	Caldesmon 1
<i>CAV2</i>	Caveolin 2
<i>EGFR</i>	Epidermal growth factor receptor (erythroblastic leukemia viral (v-erb-b) oncogene homolog, avian)
<i>FN1</i>	Fibronectin 1
<i>ITGB1</i>	Integrin, beta 1 (fibronectin receptor, beta polypeptide, antigen CD29 includes MDF2, MSK12)
<i>JAG1</i>	Jagged 1 (Alagille syndrome)
<i>MSN</i>	Moesin
<i>MST1R</i>	Macrophage stimulating 1 receptor (c-MET-related tyrosine kinase)
<i>NODAL</i>	Nodal homolog (mouse)
<i>PDGFRB</i>	Platelet-derived growth factor receptor, beta polypeptide
<i>RAC1</i>	RAS-related C3 botulinum toxin substrate 1 (Rho family, small GTP binding protein RAC1)
<i>STAT3</i>	Signal transducer and activator of transcription 3 (acute-phase response factor)
<i>TGFB1</i>	Transforming growth factor, beta 1
<i>VIM</i>	Vimentin
Cytoskeleton	
Symbol	Name
<i>CAV2</i>	Caveolin 2
<i>KRT7</i>	Keratin 7
<i>MAP1B</i>	Microtubule-associated protein 1B
<i>PLEK2</i>	Pleckstrin 2
<i>RAC1</i>	RAS-related C3 botulinum toxin substrate 1 (Rho family, small GTP binding protein RAC1)
<i>VIM</i>	Vimentin
Extracellular matrix and cell adhesion	
Symbol	Name
<i>BMP1</i>	Bone morphogenetic protein 1
<i>BMP7</i>	Bone morphogenetic protein 7
<i>CDH1</i>	Cadherin 1, type 1, E-cadherin (epithelial)
<i>CDH2</i>	Cadherin 2, type 1, N-cadherin (neuronal)

continued